Molecular crosstalk between the endophyte Paraconiothyrium variabile and the phytopathogen Fusarium oxysporum -modulation of lipoxygenase activity and beauvericin production during the interaction

Margot Bärenstrauch, Stéphane Mann, Chloé Jacquemin, Sarra Bibi, Oum-Kalthoum Sylla, Emmanuel Baudouin, Didier Buisson, Soizic Prado, Caroline Kunz

Molecular crosstalk between the endophyte *Paraconiothyrium variabile* and the phytopathogen *Fusarium oxysporum* – modulation of lipoxygenase activity and beauvericin production during the interaction

Margot Bärenstrauch[a,1], Stéphane Mann[a], Chloé Jacquemin[a], Sarra Bibi[a], Oum-Kalthoum Sylla[a], Emmanuel Baudouin[b], Didier Buisson[a], Soizic Prado[a], Caroline Kunz[a,c,*]

[a] Muséum National d'Histoire Naturelle, Unité Molécules de Communication et Adaptation des Micro-organismes, UMR 7245, CP 54, 57 Rue Cuvier, 75005, Paris, France

[b] Sorbonne Université, CNRS UMR7622, Institut de Biologie Paris-Seine-Laboratoire de Biologie du Développement (IBPS-LBD), 75005 Paris, France

[c] Sorbonne Université, Faculté des Sciences et Ingénierie, UFR 927, F-75005 Paris, France

[1] Present address : UMR 5600 EVS-ISTHME, IUT de Saint-Etienne, Campus Métare - 28 RUE Léon Jouhaux, 42023 SAINT-ETIENNE CEDEX 2

[*]Corresponding author. e-mail address: caroline.kunz@upmc.fr

ABSTRACT

Plants comprise many asymptomatic fungal endophytes with potential roles of plant protection against abiotic and biotic stresses. Endophytes communicate with their host plant, with other endophytes and with invading pathogens but their language remains largely unknown. This work aims at understanding the chemical communication and physiological interactions between the fungal endophyte *Paraconiothyrium variabile* and the phytopathogen *Fusarium oxysporum*. Oxylipins, common means of communication, such as 13-hydroperoxy-9,11-octadecadienoic acid (13-HPODE), had been shown in our earlier studies to be overproduced during dual culture between the two fungal antagonists. On the other hand, the mycotoxin beauvericin was reduced in the interaction zone. The present work addresses the mechanisms underlying these changes. Hydroperoxy oxylipins are produced by lipoxygenases and *P. variabile* contains two lipoxygenase genes (*pvlox1* and *pvlox2*), whereas *pvlox2*, but not *pvlox1*, is specifically up regulated during the interaction and none of the *F. oxysporum lox* genes vary. Heterologous expression of *pvlox2* in yeast shows that the corresponding enzyme PVLOX2 produces 13-HPODE and, therefore, is most likely at the origin of the overproduced 13-HPODE during the interaction. Compellingly, beauvericin synthase gene *beas* expression is induced and beauvericin amounts increase in *F. oxysporum* mycelium when in contact with *P. variabile*. 13-HPODE, however, does not affect *beas* gene expression. Beauvericin, indeed, inhibits *P. variabile* growth, which counteracts and

biotransforms the mycotoxin leading to reduced amounts in the interaction zone which allows further expansion of the endophyte. In order to study the interaction between the protagonists *in planta*, we set up an *in vitro* tripartite interaction assay, including the model plant *Arabidopsis thaliana*. *F. oxysporum* rapidly kills *A. thaliana* plants, whereas *P. variabile* provides up to 85% reduction of plant death if present before pathogen attack. Future studies will shed light on the protection mechanisms and the role of oxylipins and beauvericin degradation herein with the long-term aim of using endophytes in plant protection.

Keywords : *Paraconiothyrium variabile*; *Fusarium oxysporum*; endophyte; oxylipins; lipoxygenase; beauvericin

Abbreviations : 13-oxo-9,11-octadecadienoic acid (13-oxo-ODE), 13-hydroperoxy-9,11-octadecadienoic acid (13-HPODE), 13-hydroxy-9,11-octadecadienoic acid (13-HODE), hydroperoxy octadecadienoic acid (HPODE), hydroxy octadecadienoic acid (HODE), polyunsaturated fatty acid (PUFA), Lipoxygenase (LOX), liquid chromatography mass spectrometry (LC-MS)

1. Introduction

Endophytes are microorganisms that develop asymptomatically within living plant tissues (Petrini, 1991; Wilson, 1995). Indeed, they colonize the plant interior and contribute to plant growth, development, fitness and enhanced disease resistance to pathogens (Hardoim et al., 2015; Partida-Martínez and Heil, 2011; Rodriguez et al., 2009, 2008; Vandenkoornhuyse et al., 2015). For example, the fungal endophyte *Piriformospora indica* reprograms barley to disease resistance (Waller et al., 2005) and *Fusarium equiseti* reduces root rot disease of pea (Šišić et al., 2017). These findings initiated studies using endophytes as biocontrol agents (Eljounaidi et al., 2016; Kandel et al., 2017; Latz et al., 2018). To better understand the mechanisms by which endophytes protect their ecological niche and might fight back invading phytopathogens, their chemical communication with the plant host, but also with co inhabiting endophytes and aggressive phytopathogens is of special interest.

Our team isolated fungal endophytes (Langenfeld et al., 2013) of the conifer *Cephalotaxus harringtonia* (Japanese Plum Yew), and further analysed their functional diversity (Combès et al., 2012). The Dothideomycete *Paraconiothyrium variabile* shows inhibitory effect on the *in vitro* growth of various phytopathogens including *Fusarium oxysporum* which causes vascular wilt disease in over 100 different plant species including conifers (Dean et al., 2012; Michielse and Rep, 2009). Moreover, our investigations showed that *P. variabile* specifically metabolizes the host plant

metabolome to the benefit of its own growth (Tian et al., 2014), produces anti bacterial, original eremophilanes (Amand et al., 2017) and hydrolyzes surfactins of co isolated *Bacillus subtilis* bacteria (Vallet et al., 2017).

Metabolomic investigations of the *in vitro* interaction between *P. variabile* and the phytopathogen *F. oxysporum* revealed competition induced metabolite production (Combès et al., 2012). During co inoculation experiments confronting the two fungi on agar medium, the two oxylipins (Fig. 1C), 13-oxo-9,11-octadecadienoic acid (13-oxo-ODE) and 13-hydroperoxy-9,11-octadecadienoic acid (13-HPODE) were overproduced, whereas beauvericin (Fig. 1C), a mycotoxin from *F. oxysporum,* was present in lower amounts in the interaction zone as compared to single culture. Beauvericin is a virulence factor in *F. oxysporum* and is biosynthesized by a non ribosomal peptide synthetase, encoded by the *beas* gene (López-Berges et al., 2013).

Oxylipins constitute a large family of oxidized fatty acids and metabolites derived therefrom which show diverse signalling properties in mammals, microbes and plants (Christensen and Kolomiets, 2011; Fischer and Keller, 2016; Tsitsigiannis and Keller, 2007; Wasternack et al., 2013). Fungi produce a wide diversity of oxylipins (Brodhun and Feussner, 2011; Noverr et al., 2003) and have been mostly studied in *Aspergillus* where they serve as intra species extracellular signals to regulate spore development, mycotoxin production (Rodriguez et al., 2008; Scarpari et al., 2014) and quorum sensing (Affeldt et al., 2012; Horowitz Brown et al., 2008). The production of cross kingdom signalling oxylipins by pathogenic fungi modifying plant and mammalian host responses has also been documented in recent years (Brodhun and Feussner, 2011; Christensen and Kolomiets, 2011; Fischer and Keller, 2016; Pohl and Kock, 2014) but their role within the plant microbiota and in particular in endophyte - phytopathogen interactions remains unexplored. Oxylipins are biosynthesised by a variety of oxygenases incorporating oxygen into polyunsaturated fatty acid (PUFA) substrates (Brodhun and Feussner, 2011; Fischer and Keller, 2016). Lipoxygenases (LOXs; EC 1.13.11.12), non haem iron or manganese containing dioxygenases catalyse the conversion of PUFAs to fatty acid hydroperoxides such as 13-HPODE (Ivanov et al., 2010; Oliw, 2002) and are therefore good candidates to be at the origin of the up regulated oxylipins during *P. variabile* – *F. oxysporum* interaction.

The objective of this work was to investigate if the expression of a specific *lox* gene of *P. variabile* or *F. oxysporum* is enhanced during their interaction, and if so, if this gene codes for a functional LOX producing 13-HPODE. Regulation of beauvericin production via 13-HPODE or the endophyte itself was then studied. Beauvericin down regulation might be in the interest of

the endophyte and its growth inhibitory activity towards *P. variabile* was thus elucidated as well as the physiological response of the endophyte to the presence of the mycotoxin. A newly developed *in vitro* tripartite interaction assay, including the model plant *Arabidopsis thaliana*, allowed testing plant protection from *F. oysporum* disease in the presence of *P. variabile*.

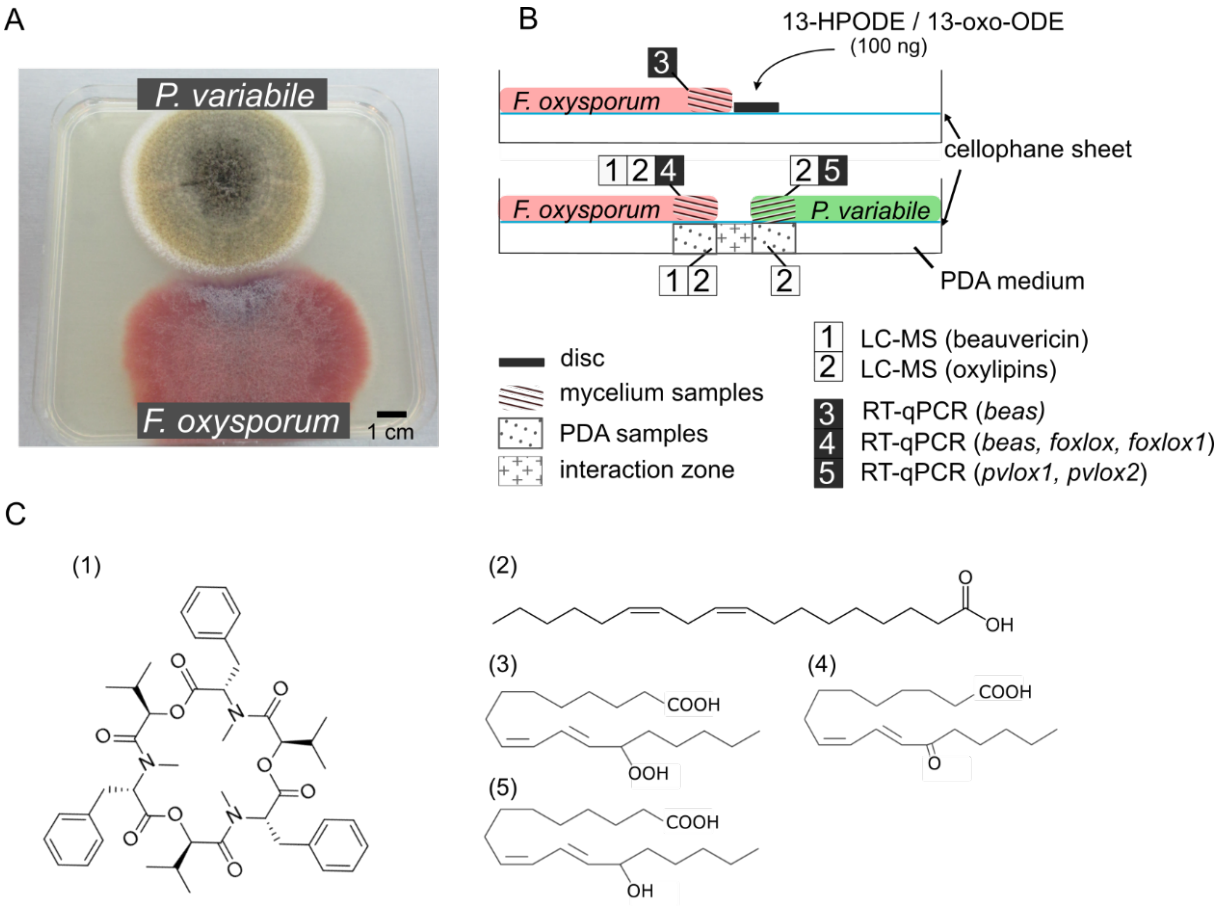

Fig. 1. Experimental design for dual culture experiments. (A) Co-culture on PDA of *P. variabile* and *F. oxysporum* just before sampling for RT-qPCR and mass spectrometry (LC-MS) analyses. Control conditions correspond to each fungus grown alone. (B) Diagrams showing the experimental designs. Above, approach to test *beas* gene induction in the presence of oxylipins; below, approach to test *beas* and lox gene expression, as well as beauvericin and oxylipin measurements in co-culture. The diagrams depict cross-sections of *in vitro* cultures on PDA indicating sampling zones and the type of analysis for which they are intended. To measure the effect of oxylipins on beauvericin synthesis, a disc soaked with 13-HPODE, 13-oxo-ODE or ethanol (control) was added in front of the mycelium (diagram above). The mycelium was collected to assess *beas* gene expression by RT-qPCR. For co-culture experiments (below), the mycelia of both fungi were collected to assess *beas* and *lox* gene expressions by RT-qPCR. Mycelium and medium samples were collected to quantify beauvericin and oxylipins by LC-MS. (C) Structures of beauvericin (1), linoleic acid (2), 13-HPODE (3), 13-oxo-ODE (4) and 13-HODE (5).

2. Materials and methods

2.1. Filamentous fungal strains and culture conditions

A monospore strain, MS1, derived from the endophyte *Paraconiothyrium variabile* isolated from the conifer tree *Cephalotaxus harringtonia* (Langenfeld et al., 2013) was used. *P. variabile* is conserved in the fungal culture collection of the National Museum of Natural History in Paris, under the identifier LCP5644. The strain *Fusarium oxysporum f. sp. medicaginis* is conserved in the same collection under the identifier LCP531. Both microorganisms were maintained on PDA solid medium (Potato Dextrose Agar Difco, CONDA: potato starch 4 g L^{-1}, dextrose 20 g L^{-1}, agar 15 g L^{-1}, pH 5.6). Nephelometry assays were performed using PDB medium (Potato Dextrose Broth, CONDA: infusion from potatoes 26.5 g L^{-1}, pH 5.6). For RT-qPCR and metabolite extractions, strains were cultivated on PDA medium on Cellophane sheets (Hutchinson) as shown in Fig. 1. For dual cultures, spores from *P. variabile* were obtained from a 20 to 30-day old culture and 5 µL (10^5 spores ml^{-1}) of this suspension was inoculated at 2.5 cm from the Petri dish edge. *Fusarium oxysporum* inoculum was prepared in the same way from a 7-day old culture and inoculated seven days later at 2.5 cm from the Petri dish edge opposite *P. variabile* mycelium.

2.2. Chemicals

A stock standard solution of beauvericin (BEA) was purchased from Cayman and kept at -20°C at a concentration of 1 mg mL^{-1} in DMSO or methanol. Commercial solutions of (±)13-hydroperoxy-9*Z*,11*E*-octadecadienoic acid and 13-oxo-9*Z*,11*E*- octadecadienoic acid were purchased from Cayman and stored at 100 µg mL^{-1} in ethanol at -80°C, linoleic- and linolenic acid from Sigma.

2.3. Reverse-transcriptase quantitative PCR (RT-qPCR)

2.3.1. Experimental design and samples

Mycelium samples of *P. variabile* and *F. oxysporum* from three biological repetitions were collected as illustrated on Figure 1B. For each condition (fungus alone or in co culture), 30 to 100 mg of fresh mycelium were pooled from two distinct Petri dishes. Samples were kept frozen at -80°C for no more than a month before being processed. Samples were grinded in liquid nitrogen and extracted with the Rneasy Plant Mini kit (Qiagen). Extracted RNA (~ 5 µg) was treated with the DNAse Max kit from MOBIO (#15 200-500) for 1h at 37°C, according to the furnisher's

instructions. RNA quality was assessed by migration on agarose gel and determination of the A260/280 ratio using a spectrophotometer (Nanovue Plus CE Healthcore). The same apparatus was used to quantify the extracted RNA. Resulting RNAs were reverse transcripted on the same day.

2.3.2. Reverse transcription

Total RNA (400 ng for *F. oxysporum* and 600 ng for *P. variabile*) was reverse transcripted using 1 µL of RevertAid reverse Transcriptase (Thermo Fischer scientifc, #EP0441), 4 µL of random hexamers at 50 µM (Invitrogen), 8 µL of reaction buffer 5x, 1 µL of Ribolock RNAse inhibitor (Thermo Fischer Scientific #E00381) and 4 µL of dNTPs at 10 mM (Thermo Fischer Scientific #R0191) in a final volume of 20 µL. The thermocycler program included a preliminary step of 10 minutes at 25°C, followed by 60 minutes at 42°C and a final step of 10 minutes at 70°C to inactivate the reverse transcriptase. Finally, the resulting cDNA were diluted 1:10 with MilliQ water and stored no longer than two weeks at -20°C. In order to assess for genomic DNA contamination absence, a control sample was prepared during RT step without the enzyme. The samples were then subjected to qPCR and checked on agarose gel. Moreover, to check the absence of inhibition of the RT reaction, successive dilutions of RNA were used. For *F. oxysporum*, 84, 168, 343, and 682.5 ng were tested and 100, 200, 400, 600 and 800 ng for *P. variabile*. It enabled us to ensure the linearity of the relation between the amount of RNA used in the RT reaction and the corresponding amount of cDNA detected by qPCR.

2.3.3. Quantitative PCR (qPCR)

For the relative quantification of gene expression of selected genes, specific primer pairs were designed using Primer 3 version 4.0.0 software (Supplementary table 1). Oligonucleotides were synthesized by Eurofins. qPCR reactions were performed in a final volume of 10 µL including 4 µL of cDNA diluted 1:10, 2 µL of SyberGreen I (LightCycler FastStart DNA SyberGreen I, Roche) and a 2 µL mix of reverse and forward primers at 0.25 µM each. No-template controls were included in each run for each primer pair. Capillaries and a Light Cycler 2.0 instrument were from Roche. The thermocycler program is given in Supplementary table 2. Each run was performed twice, with two technical replicates for each sample. To estimate amplification efficiency of primers, different dilutions ranges were prepared in sterile deionized water depending on gene expression levels and standard curves were performed in duplicates (Supplementary table 3). Primers specificity was assessed by checking the melting curves and making qPCR products migrate on agarose gel. Data were analyzed with R 3.5.0 according to the method described before (Hellemans et al., 2007). Data are presented as the log2 derived fold

change normalized by the corresponding fold change for reference genes. Log2 fold changes were considered significant when above 1 or below -1.

2.4. Extraction of metabolites in coculture

For coculture experiments, mycelium from *F. oxysporum* and *P. variabile* in coculture or grown alone was collected as illustrated on Figure 1B from two Petri dishes and pooled to reach around 100 mg of wet mycelium mass. Microorganisms grew until they came into contact before collecting the samples. Three agar plugs from the same two Petri dishes with a 0.3 cm diameter die cutting were pooled and used as controls. Samples were frozen and kept at -80°C before beauvericin and oxylipin extraction.

2.4.1. Beauvericin

Mycelium samples from *F. oxysporum* or PDA samples (secreted fraction) collected underneath the mycelium (Fig. 1B) were crushed in a mortar with liquid nitrogen and the powder was transferred in glass tubes with 2 mL of distillated ethyl acetate. After 20 minutes of sonication, samples were centrifugated 10 minutes at 4°C and 4000 rpm. The extraction was performed twice and the collected supernatants were evaporated using a SpeedVac at 40°C. Crude extracts were kept dried at -20°C before LC-MS analyses. Samples were solubilized in 100 µL of methanol and 2 µL injected in the HPLC-MS to detect beauvericin.

2.4.2. Oxylipins

Mycelium samples from *P. variabile* and *F. oxysporum* or PDA samples (secreted fraction) collected underneath the mycelium (Fig. 1B) were crushed in a mortar with liquid nitrogen and the powder was transferred in glass tubes with 1.5 mL of hexane: isopropanol (3:2) added with 0.5 mL of MilliQ water. After a 25-minute sonication in cold water, samples were centrifuged 10 minutes at 4°C and 4000 rpm and the hexane layer collected. The extraction was performed twice and the extracts were evaporated using a SpeedVac at room temperature. Crude extracts were kept dried at -20°C before LC-MS analyses. Samples were solubilized in 30 µL of methanol and 4 µL injected in the HPLC-MS to detect 13-HPODE and 13-oxo-ODE.

2.5. LC/MS quantification

Samples were analyzed by liquid chromatography (Ultimate 3000, ThermoScientific) coupled to a high resolution Quadrupole-Time of Flight (Q-TOF) hybrid mass spectrometer (maxis II ETD, Brucker), equipped with an electrospray ionization source (ESI). The

chromatographic separation was carried out by reverse phase liquid chromatography using an Acclaim RSLC Polar Advantage type III column (2.1 x 100 mm, 120 Å) (Dionex). Optimum separation was achieved with a gradient elution using MilliQ water with 0.1% (v/v) formic acid (A) and acetonitrile containing 0.07% (v/v) formic acid (B). The separation was achieved with a flow rate of 300 µL min^{-1} and the following gradient: 5% B during 9 minutes, 50% B during 6 mn, 90% B during 4 minutes, 5% B during 2 minutes. Samples of *F. oxysporum* for beauvericin detection were acquired in positive mode. The optimal ionization source working parameters were: nebulizer 2.4 bar, temperature 200°C, capillary voltage 3500 V. Full scan mass spectra were performed from 50 to 1500 *m/z* at 5 spectra/sec. All oxylipin samples were acquired in negative mode with slight parameters modifications: capillary voltage was set to 2500 V, *m/z* range was 50-1200 with focus active. MS/MS spectra were recorded automatically and the total cycle time was 3 seconds. Commercial beauvericin and oxylipins (13-HPODE and 13-oxo-ODE) were injected to establish the retention times of the compounds and clusters of sodium-formate were used for calibration. Data were analyzed with the software Bruker Compass DataAnalysis 4.3.

2.6. Heterologous expression of PVLOX2 in Escherichia coli and Saccharomyces cerevisiae

2.6.1. Strains and media

All *E. coli* strains were cultured in LB medium with appropriate antibiotics.

The *E. coli* TOP10 strain (Invitrogen) genotype: *F- mcrA Δ(mrr-hsdRMS-mcrBC) Δ80lacZΔM15 ΔlacX74 nupG recA1 araD139 Δ (ara-leu)7697 galE15 galK16 rpsL(Str^R) endA1λ*□□□□ used for the construction of the expression vectors.

The *E. coli* BL21 (DE3) codon plus RIPL, genotype: str, B F$^-$ *ompT gal dcm lon hsdS$_B$*($r_B^- m_B$) λ(DE3 [*lacI lacUV5-T7p07 ind1 sam7 nin5*]) [*malB*]$_{K-12}$(λ^2) pLysSRARE[*T7p20 ileX argU thrU tyrU glyT thrT argW metT leuW proL ori*$_{p15A}$](Cm^R) was used for protein expression.

The *S. cerevisiae* strain CY123 was used in this study (originally from R. Kornberg laboratory, gift from J.B Boulé): *MATa, can1, ade2, trp1, ura3-52, his3, leu2-3, pep4::HIS3, prb1::LEU2, bar1::hist, lys2::pGAL1/10-GAL4*. Untransformed strain was maintained on YPD (1 % yeast extract, 2 % peptone, 2 % glucose) medium. Transformed cells were maintained in selective SCD medium supplemented with uracil (6.7 g.L^{-1} Difco Yeast nitrogen base without amino acids (Sigma Y0626), 1.92 g.L^{-1} Ura, His, Leu, Trp Drop-out mix (Sigma Y2001), 2 % glucose) medium.

2.6.2. Plasmids (Table 1)

The vector pET28a (Novagen) harbouring kanR gene was used for cDNA cloning. The cloning region carries an N-terminal or C-terminal His-Tag. The plasmid harbors the *kan*R gene.

The shuttle vector pESC containing an origin of replication in *Escherichia coli* (*ori*) and *S. cerevisiae* (2μ) was used as expression vector in yeast. This plasmid contains a gene for antibiotic resistance *Amp*R, which is used to select transformants in bacteria, and the auxotrophic marker gene *trp1* that allows selection of yeast transformants. The plasmid contains the GAL1-10 activating sequence including the transcriptional start sites for *GAL1* and *GAL10*.

Table 1. Plasmids

Plasmid	Description	Source
pET28a	N-terminal His-Tag, *kan*R	Novogen
pESC	Shuttle vector, *Amp*R, *trp1*	Gift from J.B Boulé
pMB3	pET28a containing *pvlox2* cDNA	This study
pSBS2C1	pESC containing *pvlox2* cDNA	This study

2.6.3. Isolation of total RNA and cDNA synthesis

Mycelium was collected as described for RT-qPCR experiments. Around 100 mg of mycelium was grinded in liquid nitrogen and transferred in 1 mL of TRIzol ® (Life Technologies, 15596-026). RNA was extracted using TRIzol reagent following the manufacturer's recommendations. Extracted RNA (~ 5 μg) was treated with the DNAse Max kit from MOBIO (#15 200-500) for 1h at 37°C, according to the furnisher's instructions. First strand cDNA was synthesized as described in part 2.3.2 with slight modifications: 5 μL of RNA were reverse transcripted using 2 μL of oligo(dT) at 50 μM, 4 μL of reaction buffer, 0.5 μL of Ribolock RNAse inhibitor, 2 μL of DNTPs. The final step at 70°C was removed to avoid degradation of long cDNA.

2.6.4. Cloning of *P. variabile pvlox2*

Pvlox2 gene was first cloned into the pET28a vector using *in vivo* cloning method as described by Zhu *et al.* (Zhu et al., 2010) with TOP10 *E. coli*. For that, *pvlox2* was amplified from 1 μL of undiluted cDNA with the HighFidelity Phusion polymerase (ThermoFischer) in a final volume of 20 μL using primers 32/33 (supplementary table 4). pET28a was amplified with

Phusion polymerase from 2.5 ng of extracted plasmid with primers 34/35 in a final volume of 100 µL. Primers 34 and 35 contain tails homologous with *pvlox2* sequence. All PCR products were purified with the Nucleospin ® PCR clean-up kit from Macherey-Nagel according to the manufacturer's instructions. To obtain PVLOX2 recombinant protein, *E. coli* TOP10 competent cells were cotransformed with 250 ng of *pvlox2* PCR product and 50 ng of linearized pET28a. The resulting plasmid pMB3 produces a recombinant protein that is fused in the N-terminal region with a Histidine tag. For production of *pvlox2* in *E. coli*, pMB3 was transformed into the expression strain BL21 (DE3) codon+.

For expression of *pvlox2* in yeast, *pvlox2-his-tag* was amplified by PCR from the pMB3 vector using the primers 220/222 (Supplementary table 4). At each extremity 30 bps identical to the pESC vector were introduced allowing assemblage with linearized pESC vector. The latter was linearized using PCR primes 213/223. PCR fragments obtained were co-transformed with *E. coli* TOP10 and the plasmid pSBS2C1 obtained by homologous recombination (Zhu et al., 2010).

2.6.5. Expression and purification in yeast

The plasmid pSBS2C1 was transformed into CY123 yeast strain using a standard lithium acetate protocol (Hill et al., 1991) and transformed clones were selected on SCD-Trp medium. For heterologous expression of the PVLOX2 his-tag protein, the protocol of Burges was applied (Burgers, 1999). Transformed cells were grown initially under conditions selective for the plasmid (-Trp) in complete minimal medium until mid-log phase. Cells were then diluted with an equal volume of nonselective rich medium to boost the metabolic rate of the cells. Galactose (2 %) was then added to this medium to induce expression over night. Yeast cells were recuperated by centrifugation, resuspended in an equal volume of two times concentrated lysis buffer (0.6 M NaCl, 0.1 M NaH_2PO_4, 20 mM imidazole) and ground in liquid nitrogen. After unfreezing and centrifugation of the ground yeasts, the supernatant (soluble fraction) was recuperated and a protease inhibitor mix (PNSF 0.5 mM, $NaHSO_3$ 10 mM, Leupeptine 1 µM, Pepstatine 1 µM) added to the cells (1µL per 100µL of sample). The soluble fraction was then loaded on a column containing 2 mL of His Select HF Nickel affinity resin (Sigma H0537) kept at 4 °C. Bound proteins were eluted with successive elution steps using 50 mM, 100 mM and 250 mM imidazole in 1x lysis buffer. Imidazole was removed from the samples applying them to a Sephadex G-25 column. Proteins were analysed using 10 % SDS-PAGE and Western blotting. Blots were probed with monoclonal anti Histidine antibody (SIGMA H1029) and an alkaline phosphatase conjugated secondary antibody (BETHYL A90-238AP). The revelation was done with a chemioluminescent substrate (BioRad, 170-5018) and luminescent bands read with a transluminator (Fusion Fx7).

2.7. LOX activity

LOX activity was assayed using purified PVLOX2 protein, or soluble fraction, using 250 µg of the substrate linoleic acid (Fig. 1C) in 1 mL 50 mM (Tris)/HCL-buffer, pH 8.0 containing 10 % glycerol and 125 mM NaCl (Brodhun et al., 2013). Samples were incubated for 30 minutes at room temperature and reactions stopped with methanol. Fatty acid derivatives were extracted with 1 mL $CHCl_3$. The $CHCl_3$ phase was filtered through a Pasteur pipette containing cotton swab and magnesium sulphate to eliminate all traces of water left. The recuperated phase was dried under a continuous argon stream and stored at -20°C before LC-MS analysis of oxylipins as described above (2.5.).

2.8. Nephelometry assays

Spores of *P. variabile* were collected by grinding a 1 cm^2 piece of mycelium from a 20-day-old culture in 1 mL of glycerol 25%. Spores were filtered on bolting clothes (25 µm and 10 µm) and the suspension was adjusted by counting spores in a hemocytometer cell counting chamber. A spore suspension at 10^5 or 10^3 spores mL^{-1} in 300 µL PDB was poured in each well of a 96-well plate (Falcon). Beauvericin was added at a final concentration of 100 µg mL^{-1} with 1% DMSO. For controls, *P. variabile* grew in PDB medium in the presence of 1% DMSO. Growth was automatically recorded for 72h at 25°C using a nephelometric reader (NEPHELOstar Galaxy, BMG Labtech, Offenburg, Germany), equipped with a 635-nm laser source (Joubert et al., 2010). The 96-well plates were subjected to double orbital shaking at 400 rpm for the whole incubation period. Measurements were done every 20 minutes with a laser intensity of 40%. Each well was measured for 0.5 s with a laser beam focus of 2.5 mm. The experiment was repeated with three independent biological repetitions, with 6 technical replicates for each condition. Data were exported from Nephelostar Mars data software in ASCII format and further processed in R 3.5.0. Maximal growth rate (defined as the highest slope) and time to reach maximal growth rate variables were calculated from the growth curves using the first derivative. In order to compare growth curves, the mean of the initial ten measurements was subtracted from each curve value. Means and standard errors where calculated from the replicates and a statistical analysis was performed to compare growth parameters in the presence or in the absence of beauvericin.

2.9. Biodegradation of beauvericin

A 96-well plate was prepared as described in 2.8. Controls were carried out by adding beauvericin at a final concentration of 100 µg mL^{-1} in 300 µL of PDB. The whole content of a well (mycelium and PDB medium) containing either mycelium of *P. variabile* and beauvericin or beauvericin alone was collected at different time points of incubation (0 h, 25 h, 49 h and 96 h). Extractions were performed in duplicates. Samples were extracted with 500 µL of distilled methanol, sonicated for 30 minutes and kept at 4°C before LC-MS analysis. Samples were diluted 1:100 in methanol and 1 µL was injected in the HPLC-MS for beauvericin quantification.

2.10. Plant assays

2.10.1. Plant protection assay

Arabidopsis thaliana Col-0 seeds were surface sterilized by immersion in a mixture of 40 mL absolute ethanol and 10 mL 0,75 % NaOCl for 10 minutes under occasional stirring. Seeds were then rinsed five times for one minute in absolute ethanol and dried in an open eppendorf under sterile conditions. Seeds were sown on a ½ MS solid medium (2.3 g Murashige + Skoog Medium, Duchefa Biochimie, 6.4 g plant agar, Duchefa Biochimie, per liter). Ten seeds evenly distributed were applied per petri dish (90 mm diameter) containing ½ MS solid medium and the petri dishes stored at 4 °C for 48 hours to break dormancy. The seeds were then incubated at 25 °C, 12 h light, 12 h dark (Day 0).

P. variabile and *F. oxysporum* spore suspensions were prepared at 10^4 spores mL^{-1} . 10 µl droplets of the spore suspensions were applied per *A. thaliana* seed. For test 1, *P. variabile* spores were inoculated on the ½ MS culture medium at the same time as *A. thaliana* seeds; *F. oxysporum* spores were applied three days after incubation of the seeds at 25 °C (Day 3). For test 2, *P. variabile* and *F. oxysporum* spore droplets were applied three days after incubation of the seeds at 25 °C (Day 3). For test 3, *P. variabile* spores, *F. oxysporum* spores and *A. thaliana* seeds were inoculated at the same time on the ½ MS culture medium (Day 0). For each test, seeds were inoculated without fungi (control), with *P. variabile* alone or *F. oxysporum* alone, or with both fungi. Healthy plants were counted at the moment when *F. oxysporum* had killed all the plants (= day D). For test 1 and 2, 40 plants were analysed per condition and for test 3, 20 plants were analysed. An ANOVA statistic analysis was used to determine significantly different values of healthy plants.

Infected seedlings were cut into two halves, the aerial part (hypocotyl and cotyledons) and the root, and surface sterilised in 70 % ethanol (one minute) followed by 0,4 % NaOCl (two minutes) and three rinses (three minute each) in sterile water. Surface sterilised plant parts where

then plated on PDA medium and the appearance of fungal mycelium observed over time. The mycelium could be identified as *P. variabile* 10 - 14 days post inoculation with the appearance of typical pycnides.

2.10.2. Phytotoxicity assay

Surface sterilized *Arabidopsis thaliana* seeds were sown in 96-well plates and incubated at 22°C under continuous light (150 $\mu E.s^{-1}.m^{-2}$), in the presence of 200 µL half-strength MS medium. After 7 days, the medium was removed and replaced by 200 µL of fresh medium supplemented with proper concentrations of beauvericin dissolved in DMSO. For all conditions, the final concentration of DMSO represented 1% of the total volume of medium. After 96 h, plantlets were photographed and phytotoxicity was assessed by the absence of chlorophyll pigmentation.

2.11. Bioinformatics

2.11.1. LOX sequence retrieval and phylogenetic tree construction

LOX amino acid sequences were retrieved from the protein database NCBI using the R package « rentrez 1.2.1 » (Winter, 2017). Proteins with the tag « lipoxygenase » and « fungi » as organisms were chosen. A filter was added to delete sequences having the following tags: partial, hypothetical, putative, predicted, uncharacterized, related to, unnamed, XP. We then selected proteins according to their sequence content with a custom R script inspired from Heshof *et al.,* (Heshof et al., 2014), starting with methionine, finishing with either valine or isoleucine, containing the «W-X_2-AK » motif conserved in all described LOXs and the specific amino acids involved in the catalytic center « H-$X_{3/4}$-H » and « H-X_3-N/H/S » (Supplementary Script 1). The remaining 115 sequences were then aligned with PVLOX1 and PVLOX2 by MUSCLE in SeaView software (Gouy et al., 2010). We added manually sequences from LOXs that benefit from experimental evidence, but that were not selected with the script, probably because they are registered as hypothetical proteins in NCBI. It concerns *Fusarium oxysporum* FoxLOX (KNB01601.1) and *Magnaporthe salvinii* 9S-MnLOX sequences (CAD61974.1). Despite its terminal amino acid being and alanine, we also aligned the putative LOX1 from *Fusarium oxysporum* (KNA98118.1) described by (Brodhun et al., 2013). Sequences were trimmed manually to remove duplicates and poorly aligned sequences. Conserved blocks were selected using the Gblocks method (Castresana, 2000) implemented in SeaView with the least stringent parameters. 101 protein sequences from fungal origins were finally used to construct a phylogenetic tree in

SeaView using the BIONJ algorithm (Poisson model, 1000 bootstrap replicates). The tree was edited with Figtree software (1.4.3).

2.11.2. LOX sequence alignments

Nine protein sequences from known LOXs were aligned using MUSCLE in Seaview software (Fig. 2A). The alignment was edited with Jalview 2.10. (Genbank accession number of sequences from top to bottom: Q8X150.2, CAD61974.4, G4NAP4.2, Q4WA38.1, F9FRH4.1, KNB0160.1, BAI99788.1).

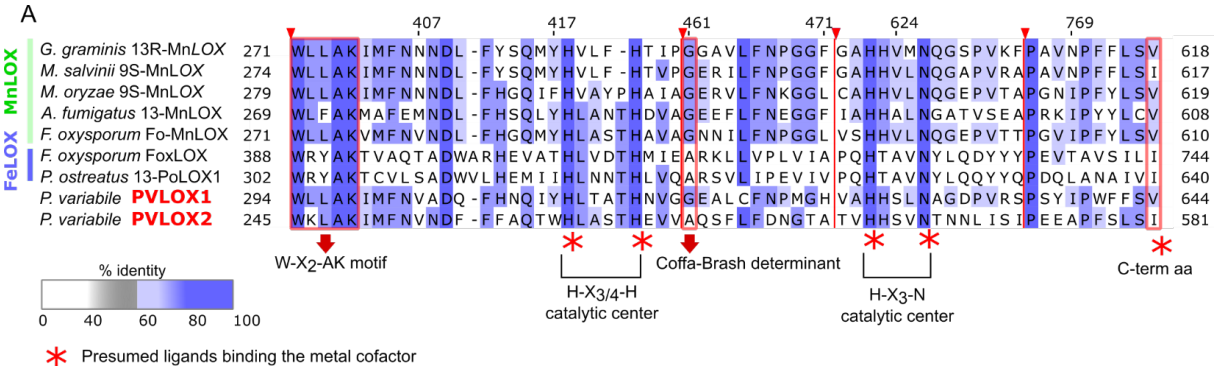

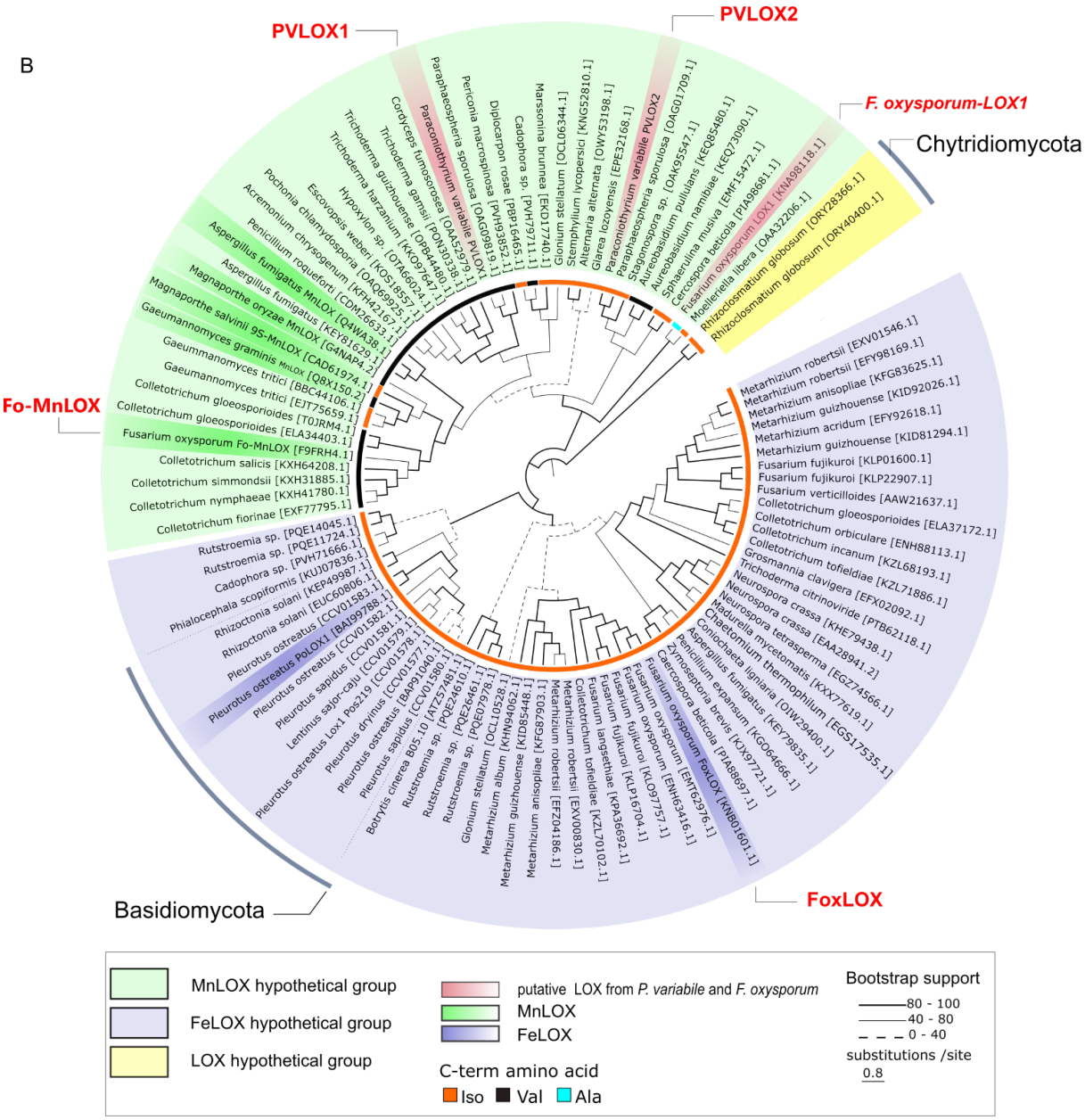

Fig. 2. *P. variabile* possesses two putative lipoxygenases. (A) Partial amino acid alignment of PVLOX1 and PVLOX2 with seven fungal LOXs biochemically characterised. Asterishks indicate the position of the five presumed ligands binding the metal cofactor (Mn or Fe). The Coffa-Brash determinant, involved in stereospecificity of LOXS, and the conserved W-X_2-AK motif are highlighted. Red arrow heads indicate the position at which sequences are shortened for graphical reasons. GenBank accession number from top to bottom: *Gaeumannomyces graminis Q8X150.2, Magnaporthe salvinii CAD61974.4, Magnaporthe oryzae G4NAP4.2, Aspergillus fumigatus Q4WA38.1, Fusarium oxysporum F9FRH4.1, Fusarium oxysporum KNB0160.1, Pleurotus ostreatus BAI99788.1.*

(B) BIONJ phylogenetic tree of 101 fungal LOX amino acid sequences including LOX from *P. variabile* (PVLOX1 and PVLOX2) and *F. oxysporum*, supported by 1000 bootstraps. Basidiomycota and Chytridiomycota phylla are highlighted, all the other sequences belong to the Ascomycota phylum. The internal circle indicates the type of amino acid present at the C-terminal position.

3. Results

3.1. P. variabile possesses two lipoxygenase genes

In order to verify if *P. variabile* is responsible for the production of 13-HPODE and 13-oxo-ODE oxylipins, we verified the presence of potential 13-LOX genes in the endophyte's genome. Sequencing of the *P. variabile* genome had been initiated before in our laboratory. BLAST searches in the genome of the endophyte using *Gaeumannomyces graminis* manganese LOX (GenBank: Q8X150.2) as template for a 13-LOX was undertaken. The purified 13*R*-manganese LOX from the cereal phytopathogen *G. graminis* had been shown before to mainly produce 13*R*-HPODE (Cristea et al., 2005; Hörnsten et al., 2002; Su and Oliw, 1998). BLAST results reveal two *P. variabile* sequences exhibiting significant similarity to the *G. graminis* 13-LOX. The two open reading frames identified show 36% and 39% identity to the *G. graminis* MnLOX and are named respectively *pvlox1* and *pvlox2*.

The C-terminal region (catalytic domain) of the two hypothetical lipoxygenases PVLOX1 and PVLOX2 were then aligned with seven other fungal LOXs (Fig. 2A), which have been characterized biochemically (Brodhun et al., 2013; Heshof et al., 2014; Kuribayashi et al., 2002; Su and Oliw, 1998; Wennman et al., 2015; Wennman and Oliw, 2013). All these LOXs form both 13-HPODE (Fig. 1 C) and 9-HPODE and sometimes 11-HPODE. Both PVLOXs contain the highly conserved motif W-X_2-AK found in all LOXs (Heshof et al., 2014), as well as the five catalytic amino acids responsible for metal binding, in other words the three histidines, the asparagine and the C-terminal valine or isoleucine amino acids. At the position of the "Coffa-Brash" determinant, a glycine or an alanine involved in the stereospecificity of LOXs (Coffa and Brash, 2004), is also present in the two PVLOXs. PVLOX1, however, has a glycine and PVLOX2 an alanine at "Coffa-Brash" determinant. Both enzymes carry a N-terminal signal sequence, and are predicted to have molecular sizes of 68 and 64 kD for PVLOX1 and PVLOX2 respectively using Expasy software, and pI values of 5,78 for both enzymes.

Alignment of PVLOX1 and PVLOX2 with 101 putative fungal amino acid LOX sequences retrieved from the protein database NCBI generated a phylogenetic tree as shown in Fig. 2B. PVLOX1 and PVLOX2 cluster together with other hypothetical and assessed manganese fungal lipoxygenases. All fungal FeLOXs included in the tree have Isoleucine as their C-terminal amino acid, whereas the corresponding amino acid in MnLOXs is Valine, or Isoleucine, with the exception of the *F.oxysporum*-LOX1 showing an alanine at the C-terminal

end. PVLOX1 differs from PVLOX2 in that it has Valine as opposed to Isoleucine at its C-terminal end.

Altogether, *P. variabile* retains two *lox* genes, *pvlox1* and *pvlox2,* coding for putative LOXs (PVLOX1 and PVLOX2) with primary structures indicating that these proteins are lipoxygenases capable of forming 13-HPODE.

3.2. Pvlox2 is specifically induced during the P. variabile – F. oxysporum interaction

To elucidate if a *F. oxysporum* LOX or a *P. variabile* LOX is at the origin of the oxylipins accumulation during their interaction, *lox* gene expression studies were conducted. First, the presence of *lox* genes in the *F. oxysporum* strain used in our study was investigated using its genome sequence available on NCBI (GCA_001652425.1). A BLAST analysis revealed the presence of three sequences exhibiting high identities (97-99%) to *fo-mnlox*, *foxlox* and *foxlox1* (Fig. 2B). These three genes were investigated using specific primers and *foxlox* and *foxlox1* gene could be amplified, but not the *fo-Mnlox* gene (data not shown).

The two fungi were grown together and mycelium samples were collected at the confrontation zone just before the two fungi were touching and used for RT-qPCR analysis (Fig. 1A, B). Results show that none of the *F. oxysporum lox* genes are significantly induced during the interaction, with *foxlox1* not expressed at all. In contrast, *pvlox*2 expression is significantly induced during co-culture whereas *pvlox1* expression pattern is identical in co culture or in control experiments (Fig. 3 A). All together these experiments show that during the antagonistic interaction between *P. variabile* and *F. oxysyporum,* only *pvlox2* is specifically upregulated.

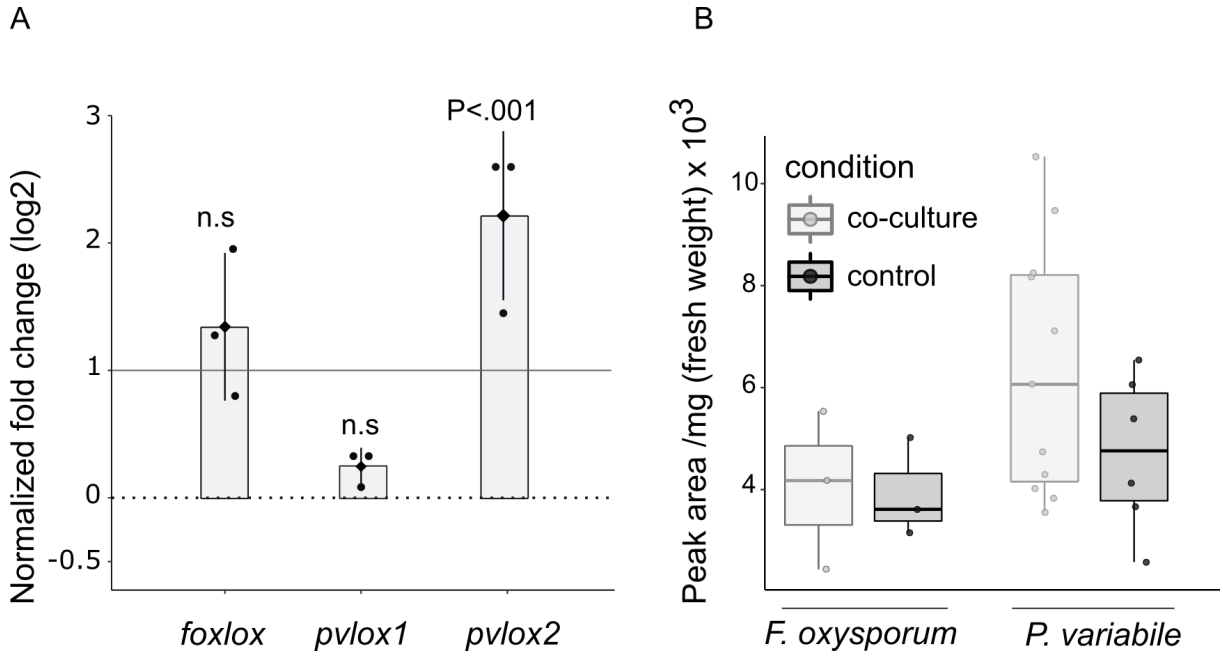

Fig. 3. Oxylipin synthesis in co-culture. (A) *Lox* gene expression in *F. oxysporum* (*foxlox* and *foxlox1*) and *P. variabile* (*pvlox1* and *pvlox2*) during co-culture versus single-culture (control condition). Gene *foxlox1* does not appear on the graph as this gene was never expressed in any conditions. Data represent the derived log2 fold changes (mean value ± SD) relative to gene expression in control conditions determined by RT-qPCR. Values are means of three biological repetitions (pictured as circles), each consisting of four technical replicates. A bootstrap analysis, conducted on the derived log2 mean, assigned significance to the fold change values with comparison to the theoretical value of 1. (B) 13-HPODE concentration detected by LC-MS (Supplementary Fig.1B) for *F. oxysporum* and *P. variabile* in co-culture versus fungi grown alone (control). Values are expressed as the peak area per mg of fresh weight, for the ion at m/z $[M\text{-}H]^-$: 311,2233 (13-HPODE).

3.3. P. variabile produces elevated 13-HPODE during the interaction with F. oxysporum

The oxylipins HPODE and oxo-ODE were extracted from mycelia of both fungi *P. variabile* and *F. oxysporum* and from the PDA culture medium below using the same experimental design (Fig. 1B) as for *lox* gene expression studies and measured by LC-MS (Supplementary Fig. 1B). The major product with a retention time of 14.4 min was identified by LC-MS/MS as 13-hydroperoxy-9*Z*,11*E*-octadecadienoic acid by comparison of its retention time and mass spectrum with the commercial standard. Whilst no other HPODE isomer was found for the peak at 14.4 min retention time, it was quantified for the different samples. In accordance with the induction of *pvlox2* in *P. variabile*, the endophyte produces more 13-HPODE when grown in co-culture than grown alone. No difference in oxylipin production is measured for *F. oxysporum* (Fig. 3B). 13-HPODE content in the culture medium underneath the mycelium of both fungi are below the detection level in our mass spectrometry approach. The oxylipin 13-HPODE can be further oxidized by lipoxygenase activity (Christensen and Kolomiets, 2011) or non-enzymatically, to the

keto form 13-oxo-ODE. However, our analysis found only traces of 13-oxo-ODE, below the quantification threshold, in the mycelium and the culture medium.

3.4. Pvlox2 codes for a 13-HPODE producing lipoxygenase

In order to verify that *pvlox2* codes for a lipoxygenase producing 13-HPODE, it was heterologously expressed. First attempts of production in *E. coli* failed, as all PVLOX2 protein is found in the inclusion bodies (Supplementary Fig. 2). We succeeded, however, to produce PVLOX2 in *S. cerevisiae*. *Pvlox2* cDNA in frame with an N-terminal hexa-histidine-tag (His-Tag), under the control of the galactose inducing promoter system was transformed into *S. cerevisiae*. His-tagged protein was purified from the soluble fraction of transformed yeast cells applying Nickel affinity chromatography. Bound fractions were eluted with imidazole and the fraction eluted at 250 mM contains a histidine-tagged protein around 70 kDa corresponding to the predicted molecular weight of 64 kDa (Fig. 4).

Imidazole free PVLOX2 was tested for lipoxygenase activity using linoleic acid as the substrate (Fig 1C). The products formed after 45 minutes of incubation correspond to HPODE (m/z [M-H]$^-$ 311.2204) and HODE (m/z [M-H]$^-$ 295.2253) (Fig. 5A). Reduction of the hydroperoxy leads to the corresponding hydroxyl fatty acid. Mass spectrum of the fragmentation of the ion m/z [M-H]$^-$ 311.2204, retention time 14.6 min (Fig. 5 B) is in accordance with the fragmentation pattern of 13-hydroperoxy-9*Z*,11*E*-octadecadienoic acid by comparison with the commercial standard (Fig. 5C). This HPODE represents the major product formed. Extracted ion chromatogram at 311.2204 shows the presence of 13-hydroperoxy-9*Z*,11*Z*-octadecadienoic acid but also 9- and 11-HPODEs as analysed by LC-MS/MS (Supplementary Fig. 3).

Altogether these results show that *pvlox2* from *P. variabile* codes for a functional PVLOX2 forming 13-HPODE oxylipin as the major product. *Pvlox2* is the only *lox* gene induced specifically during the competition with *F. oxysporum*, and most likely responsible for 13-HPODE overproduction in the interaction zone.

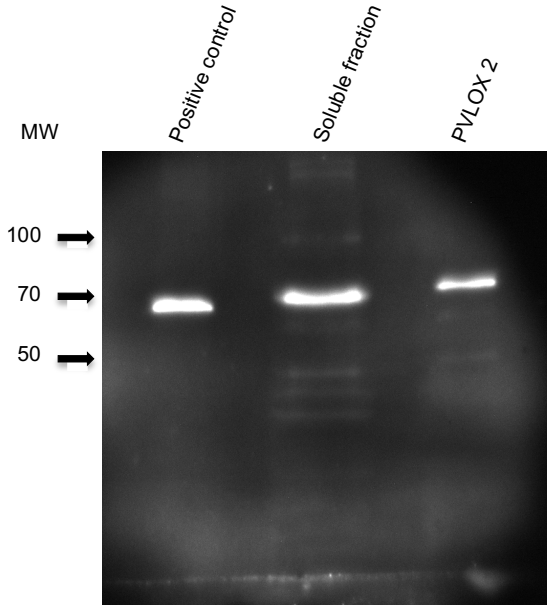

Fig 4. PVLOX2 purification. SDS-PAGE and Western Blot analysis of recombinant PVLOX2 expressed in *S. cerevisiae* after purification using nickel affinity chromatography. His-tagged proteins were detected using chimioluminescence and appear as white bands on the Western Blot. Lane 1, positive control (His-tagged PVLOX2 from *E. coli* insoluble fraction); lane 2, soluble fraction from lysed yeast cells (30 μg protein); lane 3, proteins eluted with 250 mM imidazol from the affinity column (510 ng proteins). Molecular weight standards (MW) in kDA are indicated to the left.

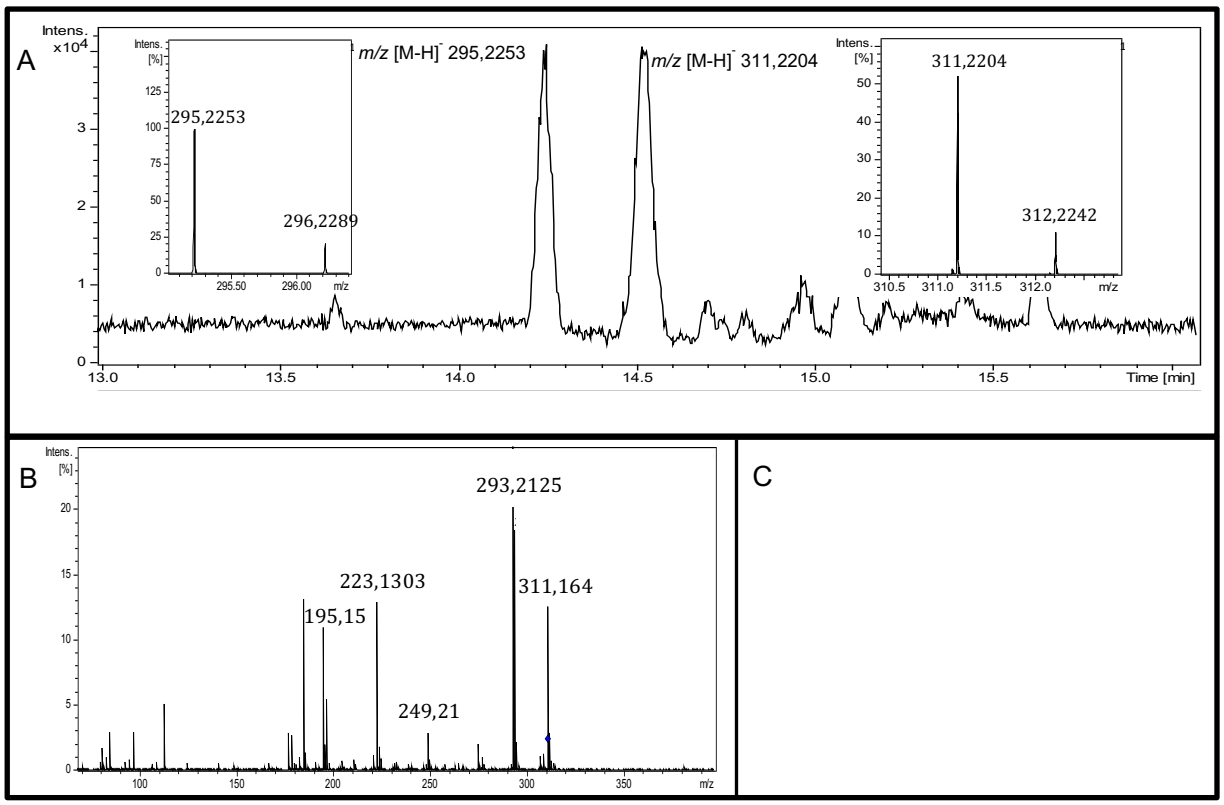

Fig. 5. PVLOX2 forms 13-HPODE. (A) LC-MS analysis of products formed from incubation of purified PVLOX2 with linoleic acid. Insets show m/z [M-H]$^-$ 295.2253 at retention time 14.22 min (HODE) and m/z [M-H]$^-$ 311.2204 at retention time 14,6 min (HPODE). (B) MS/MS spectrum of ion at m/z [M-H]$^-$ 311.2233. (C) fragmentation pattern of 13-HPODE.

3.5. P. variabile, but not 13-HPODE, enhances beas expression and beauvericin production

Our previous work (Combès et al., 2012) showed lower amounts of beauvericin in the interaction zone between *P. variabile* and *F. oxysporum* (Fig. 1B). In this work, the regulatory mechanisms for beauvericin production during the interaction were inquired. 13-HPODE as well as *P. variabile* were analysed for their potential to act as regulators of *beas* gene expression using RT-qPCR and LC/MS quantification experiments (Fig. 1B). To our astonishment, *P. variabil*e significantly up-regulates *beas* expression in *F. oxysporum,* whereas 13-HPODE nor 13-oxo-ODE influences *beas* gene expression (Fig. 6). Next beauvericin content in the *F. oxysporum* mycelium at the edge of the colony as well as in the zone below it (Fig. 1B) was quantified performing LC-MS analysis (Supplementary Fig. 1). The three independent biological repetitions show 5.4 to 24.2 fold change increase in beauvericin content in the *F. oxysporum* co culture mycelium as compared to extracts from single cultures, and a 2.5 to 14.3 fold increase in the zone below the *F. oxysporum* mycelium. These results are in concordance with the RT-qPCR results and show that the endophyte *P. variabile* induces beauvericin synthesis in *F. oxysporum* mycelium during competition. The question, thus, arose why previously we found less beauvericin in the zone between the two mycelia (Combès et al., 2012) and beauvericin transformation in the interaction zone was therefore investigated.

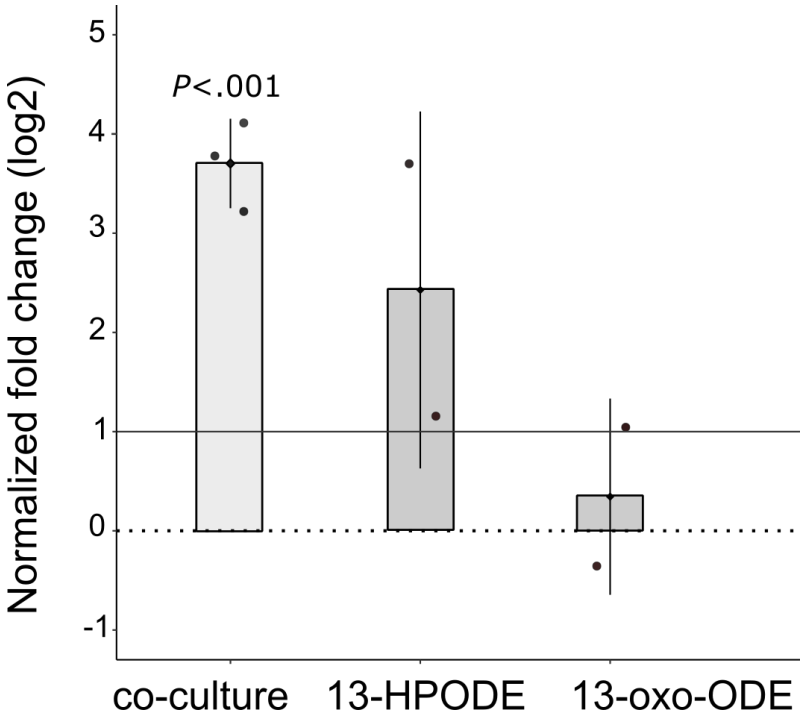

Fig. 6. Beauvericin synthetase (*beas*) gene expression in co-culture or with addition of oxylipins. Data represent the derived log2 fold changes (mean value ± SD) relative to *beas* gene expression in control condition (single-culture) determined by RT-qPCR. For co-culture experiments, values are means of 12 technical replicates from three independent biological repetitions. A bootstrap analysis conducted on the derived log2 mean assigned significance to the fold change values with comparison to the theoretical value of 1. For experiments with 13-HPODE and 13-oxo-ODE, values are means of 8 technical replicates from two independent biological repetitions.

3.6. P. variabile biotransforms beauvericin which inhibits P. variabile growth

Nephelometry tests evaluated the effect of beauvericin on the growth of *P. variabile* in the presence or absence of the mycotoxin at two initial spore concentrations (10^3 and 10^5spores mL^1). At the same time, LC-MS analysis over time estimated beauvericin concentrations in the reaction mixtures. Beauvericin delays the time to reach the maximal growth rate significantly by 13 hours (10^5 spores mL^1) and 19.3 hours (10^3 spores mL^1) (Fig. 7, Supplementary table 5). The mycotoxin also significantly reduces maximal growth rate, but only at the lower spore concentration (-14%). Beauvericin reduces maximal growth significantly by 10, respectively 23% at the two initial *P. variabile* spore concentrations. Beauvericin concentrations were followed in the test with 10^5 spores mL^{-1} and begins to decrease after 25 hours of culture, at the moment when *P. variabile* starts to grow and only 20 % of its initial concentration is left 96 hours post inoculation (Fig. 7 and Supplementary Fig. 1A and 3). Control tests show that beauvericin is not degraded during the incubation time in the absence of *P. variabile* (Supplementary Fig. 1A and 4).

These results show that beauvericin slows down the initial growth of *P. variabile,* which can then biotransform the mycotoxin and continues its growth with approximately the same speed as in the absence of beauvericin. The inhibitory effect of beauvericin is accentuated if *P. variabile* is present at a lower spore concentration in the beginning of the assay.

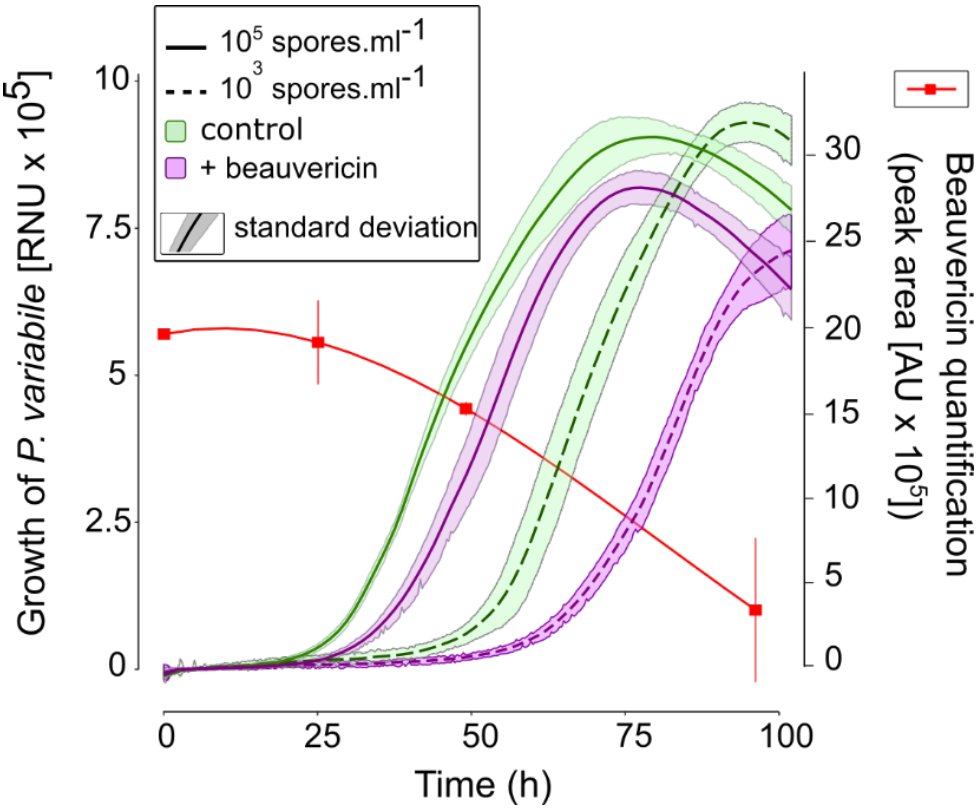

Fig. 7. Beauvericin inhibits *P. variabile* growth and the endophyte biotransforms the mycotoxin. The graph shows nephelometric growth curves of *P. variabile* at 10^5 spores.mL^{-1} or 10^3 spores mL^{-1} in a 96-well plate. Values were recorded every 20 minutes. The standard deviation values are calculated from 6 internal plate replicates. Control: *P. variabile* in PDB culture medium, + beauvericin: *P. variabile* in the presence of beauvericin at 100 µg. mL^{-1}, RNU: Relative Nephelometric Units. Beauvericin content was measured in two of the 6 replicates at different time points in the presence of *P. variabile* at 10^5 spores mL^{-1}. Values shown are the peak area for the ion at m/z=783,41 corresponding to beauvericin. AU: Arbitrary Units.

3.7. P. variabile protects young Arabidopsis plants against F. oxysporum

The endophyte *P. variabile* was tested as a protective agent of *A. thaliana* against the phytopathogen *F. oxysporum*. *A. thaliana* sterile seeds were germinated on solid medium in Petri dishes and inoculated with *P. variabile* and *F. oxysporum* at three different time points (test 1-3) of plant development (Fig. 8A). Tests were run until *F. oxysporum* had killed all the *A. thaliana* plants in the absence of *P. variabile* (day D) and the percentage of surviving plants in the presence of *P. variabile* estimated at this time point (Figure 8B). When *P. variaible* is added alone, all the plants stay healthy in all three test conditions. In test 1, when the seeds are inoculated with *P. variabile*

before *F. oxysporum*, 85 % of the plants survive. In test 2, when both fungi are applied together on germinated plants, 32 % protection is achieved in the presence of the endophyte. In test 3, both fungi are applied together with the seeds and only 10% protection is achieved in the presence of *P. variabile*. Dead cotyledons of plants infected with *F. oxysporum* alone are shown in Figure 8D, and healthy cotyledons of plants in the presence of *P. variabile* alone or in the presence of *P. variabile* and *F. oxysporum* are shown in Fig. 8C and E.

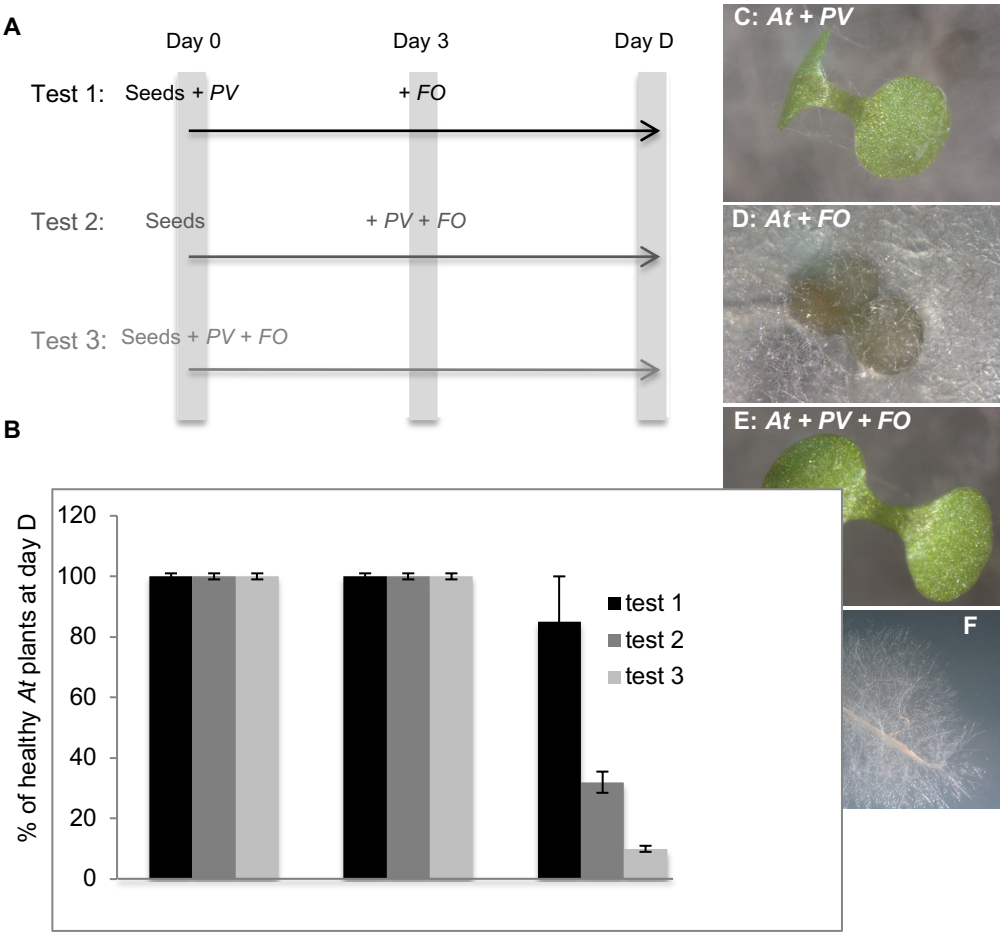

Fig. 8. Protection of *A. thaliana (At)* seedlings from *F. oxysporum (FO)* in the presence of *P. variabile (PV)*. (A) Experimental design: test 1, seeds were inoculated with *PV* at the beginning of the experiment and FO applied at day 3; test 2, *PV* and *FO* were applied together on three day old seedlings; test 3, *PV* and *FO* were applied together with the seeds. Day D is the time point when all the plants were killed by *FO* in the absence of *PV*. (B) Percentage of healthy *A. thaliana* plants was estimated at Day D in the three test conditions. Control = plants without fungi, *PV*: only *PV* applied to plants, *PV- FO*: *PV* and *FO* applied to plants. Different letters indicate significantly different values (Anova p-value<0.005, n=40 for test 1 and 2 and n=20 for test 3). (C-E) Cotyledons of *At* at day D for test 1. (F) *P. variabile* growing out from a surface sterilized stem, arrow indicates *PV* mycelium.

In order to test if *P. variabile* had entered the *A. thaliana* plants, *P. variabile* was re-isolated from surface sterilized plants. All the *A. thaliana* control plants are endophyte free, whereas in 26% of *P. variabile* inoculated plants, the endophyte can be re isolated from stems or leaves (Fig. 8F), but never from roots, indicating colonisation of the aerial part of *A. thaliana*.

Beauvericin phytotoxic activity was investigated in a standard assay on *A. thaliana* plants. As shown in Fig. 9, beauvericin at 100 µg mL^{-1} leads to a 50% mortality of treated plantlets.

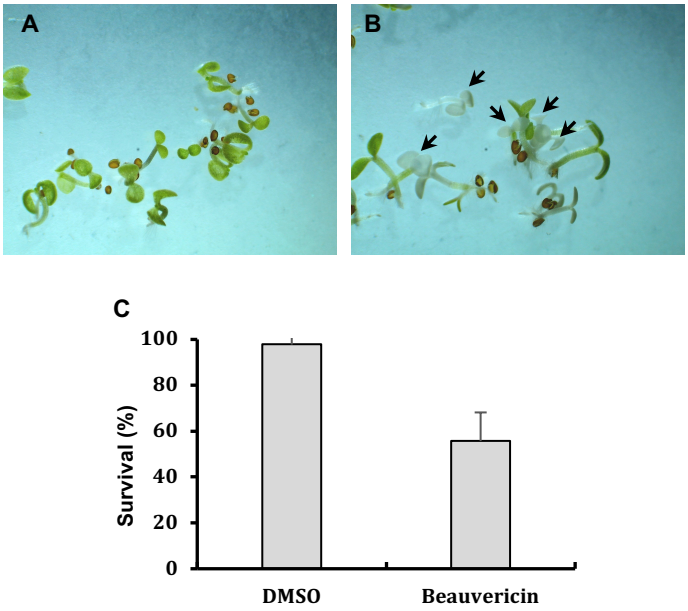

Fig. 9. Phytotoxic effect of beauvericin on *A. thaliana* plantlets. Seedlings were treated with DMSO (A) or with 100 µg.mL^{-1} beauvericin (B). Pictures represent plantlet phenotypes after 96 h of treatment and dark arrows identify dead plantlets. (C) Quantification of plantlet survival after 96 h of treatment. Results represent mean ± S.D. of three technical repeats (n=16-23 and n=26-39 seedlings for DMSO and 100 µg.mL^{-1} beauvericin, respectively).

4. Discussion

The plant biome comprises the plant and multiple microbial players, including both pathogens and mutualists and is characterized by a dense network of multitrophic interactions, which are still poorly explained. Understanding signalling and recognition processes herein are highly important for fundamental knowledge of the plant's biome functionality and thus for further potential applications such as the use of endophytes in biocontrol. Molecular communication is extensively studied in plant-pathogen interactions (Dodds and Rathjen, 2010; Peyraud et al., 2017) but only scarcely in plant-endophyte (Hardoim et al., 2015) or endophyte-phytopathogen interactions (Jonkers et al., 2012; Rodriguez Estrada et al., 2011). Functions of lipoxygenases and their oxylipins in endophytic fungi, and more particularly in interactions with

plant pathogens, have not been studied yet to our knowledge. This work identifies two *lox* genes, *pvlox1* and *pvlox2,* in the endophyte *P. variabile* showing strong identity to the *G. graminis* 13-MnLOX. During the interaction with *F. oxysporum* only *pvlox2* expression is enhanced, whereas the expression of the phytopathogen's *loxs* stays unchanged. LOX enzymes are encoded by a multi gene family and are found in mammals, plants and fungi (Brodhun and Feussner, 2011). In humans and mice, six, and in plants up to 23 LOX isoforms have been reported (Mashima and Okuyama, 2015; Upadhyay et al., 2019). While the overall structure of LOX enzymes seems to be similar, each isoform has unique properties such as substrate specificity and the expression level of each of them is differentially controlled (Costa et al., 2019; Mashima and Okuyama, 2015). In plants it has been shown that different stresses lead to differential expression of LOX family members and it is now accepted that LOX activity is a biological marker in plant stress tolerance (Babenko et al., 2017; Upadhyay et al., 2019). *Lox* gene expression in fungi-fungi interactions has not been studied yet. This work shows that *pvlox2*, but not *pvlox1,* is specifically induced in the presence of *F. oxysporum* and it might act as a stress marker in the endophyte when exposed to invading phytopathogens.

This study demonstrates that *pvlox2* is at the origin of a functional LOX named PVLOX2 that produces 13-HPODE with linoleic acid as its substrate. LOXs use iron or manganese as their metal co factor and the fungal LOXs were divided into two groups, those that encode a C-terminal isoleucine (Ile-group) and an alanine at the Coffa-Brash site or those that encode a C-terminal valine (Val-goup) and a glycine at the Coffa-Brash (Heshof et al., 2014). Biochemical analysis of several fungal LOXs identified the Ile-group as iron LOXs and the Val-group as MnLOXs (Heshof et al., 2014). PVLOX1 belongs in the Val-group. PVLOX2 is part of the Ile-group such as FoxLOX from *F. oxysporum* (Fig. 2B) for which the reaction mechanisms was characterized and iron demonstrated as the co-factor (Brodhun et al., 2013). Nevertheless, PVLOX2 aligned best with the *G. graminis* 13-*R*MnLOX belonging to the Val group using manganese as its metal ion. These observations show the interest of further biochemical analysis of PVLOXs to understand fully the structure function relationships.

Oxylipins play a role in signalling in many different cell types and as inter-kingdom signalling molecules (Battilani et al., 2018; Fischer and Keller, 2016; Pohl and Kock, 2014). 13-HPODE suppresses mycotoxin production in *Aspergillus* and it is suggested that this regulation is transcriptional (Burow et al., 1997). Our previous work showed that exogenously applied 13-oxo-ODE on *F. oxysporum* mycelium lead to a decreased production of beauvericin in the mycelium (Combès et al., 2012). 13-oxo-ODE is formed spontaneously in the presence of oxygen from 13-HPODE or by the LOX activity itself (Kühn et al., 1991). These findings rose the hypothesis

that 13-HPODE and/or 13-oxo-ODE down-regulate the *beas* gene in *F. oxysporum*. Our results, however, detect neither up- nor down-regulation of the *beas* gene in the presence of 13-HPODE or 13-oxo-ODE, indicating that these oxylipins interfer with beauvericin reduction in *F. oxysporum* mycelium in another way than transcriptional *beas* gene regulation. At the moment, we can not exclude that 9- or 11-HPODE might intervene with *beas* gene expression during the interaction. However, 13-HPODE is the major oxylipin formed during *P. variabile* – *F. oxysporum* interaction.

Interestingly, the endophyte *P. variabile* itself up-regulates *beas* gene transcription in *F. oxysporum* followed by higher beauvericine content in its mycelium and the adjacent culture medium. Moreover, the mycotoxin exerts inhibitory effect on *P. variabile* growth, indicating beauvericin production as a possible defense mechanism of *F. oxysporum* against the endophyte. Mycotoxins are defined by how they affect animals feeding on contaminating crops, but few studies question their role for the fungal fitness, both in a plant environment and in the competitive soil environment (Drott et al., 2017). Beauvericin is mostly described as a virulence factor for *F. oxysporum* needed for plant colonization (López-Berges et al., 2013) but it might also have a detrimental allelopathic effect on other microbes, helping to secure its environmental niche. Such an ecological role for mycotoxins was highlighted before (Venkatesh and Keller, 2019). Little work on beauvericin antifungal activity is present, although insecticidal, antitumor and antibacterial activity has been shown (Hamill et al., 1969; Wang and Xu, 2012). Synergistic effects of beauvericin in combination with other substances were, however, found against fungal infections in mice (Zhang et al., 2007). Beauvericin does not kill *P. variabile* and only has a growth inhibitory effect, but in presence of other environmental metabolites, potentiation of beauvericin toxicity against antagonistic microorganisms in the soil or in the plant might be possible. It has been shown that *F. fujikuroi* responds with an increase in localized production of bikaverin and beauvericin, which together show additive antibacterial activity against the invading phytobacterium *Ralstonia solanacearum* (Spraker et al., 2018)

Intriguingly, *P. variabile* counteracts and biotransforms the mycotoxin. In this way it might not only protect itself against the mycotoxin, but also other members of the microbiote and the plant host itself. Biotransformation of beauvericin by *P. variabile* also explains why in our previous work decreased levels of beauvericin were found in the interaction zone between the two fungi (Combès et al., 2012). Beauvericin is a cyclic depsipeptide with a similar cyclic core to the lipodepsipeptide surfactins, and its biotransformation by *P. variabile* is in accordance with previous results demonstrating the hydrolysis of surfactins from *Bacillus subtilis* by the endophyte (Vallet et al., 2017). These results add to the understanding on how mycotoxin levels are

regulated by microbial encounters that can offer novel insights for mycotoxin control in food and feed as stated before (Venkatesh and Keller, 2019).

The ultimate aim of this investigation is to find new means to protect plants against phytopathogens and to avoid accumulation of mycotoxins in infected plants. Thus, this work establishes an *in vitro* tripartite model system including the model plant *A. thaliana*. Outcome of tripartite interaction *in planta* has been addressed beforehand in the crop plant maize showing that pathogen (*Ustilago maydis*) aggressiveness towards the plant is lower when the endophyte (*F. verticilloides*) is present (Rodriguez Estrada et al., 2011). First results obtained in our *in vitro* tripartite system show that the presence of *P. variabile* protects *A. thaliana* plants up to 85 %. In order to obtain these results the endophyte has to be inoculated on the seedlings before the phytopathogen. This way, the endophyte can colonize the plant before pathogen attack, or simply inhibit or reduce the growth of *F. oxysporum* around the plant where it is already present. Beauvericin has been shown to induce cell death in tomato and melon protoplasts (Paciolla et al., 2004), and this study reveals its toxicity on *A. thaliana* seedlings. Beauvericin degradation might thus be another possible mechanism involved in plant protection. All these potential mechanisms need to be further explored using microscopy work to follow plant infection by the two protagonists, or genetic approaches including mycotoxin mutants of *F. oxysporum*.

In conclusion, this work further investigates the battle between the endophyte *P. variabile* and the phytopathogen *F. oxysporum* on a *in vitro* level but also in a newly established tripartite system. It shows that both fungi recognize each other leading to specific PVLOX2 induction in *P. variabile* followed by increased amounts of the signalling oxylipin 13-HPODE. How this oxylipin is interfering with *F. oxysporum* metabolisms needs to be further explored. The phytopathogen recognizes the endophyte and reacts with increased beauvericin production inhibiting the endophyte. *P. variabile*, in terms, biotransforms the mycotoxin eliminating its growth inhibitory activity. In the tripartite system including *A. thaliana*, the endophyte successfully protects its micro niche against *F. oxysporum* and at the same time diminishes plant disease.

Protein sequence accession numbers

The protein sequences reported in this article are deposited in GenBank repository: PVLOX1 (MK208825), PVLOX2 (MK208826).

Declaration of competing interest

The authors declare no conflict of interest.

Acknowledgments

The authors thank Jean-Baptiste Boulé from the laboratory "Génomique et Physiologie de l'Adaptation" at the Museum of Natural History, Paris France, for his handout of the CY123 *Saccharomyces cerevisiae* strain and the pESC plamids used in this study, as well as for his valuable technical assistance for heterologous protein expression in yeast. The authors also thank Laura Guédon, Délphine Champeval and Charlotte Garandel for their technical assistance, Soraya Chaouch for her help with RT-qPCR experiments and Arul Marie for help with the mass spectrometry. This research was supported by the ATM fund 'Microorganisms" from the Museum of Natural History, Paris France.

Appendix A. Supplementary material

Supplementary material to this article can be found online at

References

Affeldt, K.J., Brodhagen, M., Keller, N.P., 2012. Aspergillus Oxylipin Signaling and Quorum Sensing Pathways Depend on G Protein-Coupled Receptors. Toxins 4, 695–717. https://doi.org/10.3390/toxins4090695

Amand, S., Vallet, M., Guedon, L., Genta-Jouve, G., Wien, F., Mann, S., Dupont, J., Prado, S., Nay, B., 2017. A Reactive Eremophilane and Its Antibacterial 2(1H)-Naphthalenone Rearrangement Product, Witnesses of a Microbial Chemical Warfare. Org. Lett. 19, 4038–4041. https://doi.org/10.1021/acs.orglett.7b01788

Babenko, L.M., Shcherbatiuk, M.M., Skaterna, T.D., Kosakivska, I.V., 2017. Lipoxygenases and their metabolites in formation of plant stress tolerance. Ukr Biochem J 89, 5–21. https://doi.org/10.15407/ubj89.01.005

Battilani, P., Lanubile, A., Scala, V., Reverberi, M., Gregori, R., Falavigna, C., Dall'asta, C., Park, Y.-S., Bennett, J., Borrego, E.J., Kolomiets, M.V., 2018. Oxylipins from both pathogen and host antagonize jasmonic acid-mediated defence via the 9-lipoxygenase pathway in Fusarium verticillioides infection of maize. Molecular Plant Pathology 19, 2162–2176. https://doi.org/10.1111/mpp.12690

Brodhun, F., Cristobal-Sarramian, A., Zabel, S., Newie, J., Hamberg, M., Feussner, I., 2013. An

Iron 13S-Lipoxygenase with an α-Linolenic Acid Specific Hydroperoxidase Activity from Fusarium oxysporum. PLoS ONE 8, e64919. https://doi.org/10.1371/journal.pone.0064919

Brodhun, F., Feussner, I., 2011. Oxylipins in fungi: Fungal oxylipins. FEBS Journal 278, 1047–1063. https://doi.org/10.1111/j.1742-4658.2011.08027.x

Burgers, P.M.J., 1999. Overexpression of Multisubunit Replication Factors in Yeast. Methods 18, 349–355. https://doi.org/10.1006/meth.1999.0796

Burow, G.B., Nesbitt, T.C., Dunlap, J., Keller, N.P., 1997. Seed Lipoxygenase Products Modulate Aspergillus Mycotoxin Biosynthesis. MPMI 10, 380–387. https://doi.org/10.1094/MPMI.1997.10.3.380

Castresana, J., 2000. Selection of conserved blocks from multiple alignments for their use in phylogenetic analysis. Molecular biology and evolution 17, 540–552.

Christensen, S.A., Kolomiets, M.V., 2011. The lipid language of plant–fungal interactions. Fungal Genetics and Biology 48, 4–14. https://doi.org/10.1016/j.fgb.2010.05.005

Coffa, G., Brash, A.R., 2004. A single active site residue directs oxygenation stereospecificity in lipoxygenases: stereocontrol is linked to the position of oxygenation. Proc. Natl. Acad. Sci. U.S.A. 101, 15579–15584. https://doi.org/10.1073/pnas.0406727101

Combès, A., Ndoye, I., Bance, C., Bruzaud, J., Djediat, C., Dupont, J., Nay, B., Prado, S., 2012. Chemical Communication between the Endophytic Fungus Paraconiothyrium Variabile and the Phytopathogen Fusarium oxysporum. PLoS ONE 7, e47313. https://doi.org/10.1371/journal.pone.0047313

Costa, H., Touma, J., Davoudi, B., Benard, M., Sauer, T., Geisler, J., Vetvik, K., Rahbar, A., Söderberg-Naucler, C., 2019. Human cytomegalovirus infection is correlated with enhanced cyclooxygenase-2 and 5-lipoxygenase protein expression in breast cancer. Journal of Cancer Research and Clinical Oncology 145, 2083–2095. https://doi.org/10.1007/s00432-019-02946-8

Cristea, M., Engström, Å., Su, C., Hörnsten, L., Oliw, E.H., 2005. Expression of manganese lipoxygenase in Pichia pastoris and site-directed mutagenesis of putative metal ligands. Archives of Biochemistry and Biophysics, Highlight section on Redox Control of Membrane Protein Function 434, 201–211. https://doi.org/10.1016/j.abb.2004.10.026

Dean, R., Van Kan, J.A.L., Pretorius, Z.A., Hammond-Kosack, K.E., Di Pietro, A., Spanu, P.D., Rudd, J.J., Dickman, M., Kahmann, R., Ellis, J., Foster, G.D., 2012. The Top 10 fungal pathogens in molecular plant pathology: Top 10 fungal pathogens. Molecular Plant Pathology 13, 414–430. https://doi.org/10.1111/j.1364-3703.2011.00783.x

Dodds, P.N., Rathjen, J.P., 2010. Plant immunity: towards an integrated view of plant–pathogen interactions. Nature Reviews Genetics 11, 539–548. https://doi.org/10.1038/nrg2812

Drott, M.T., Lazzaro, B.P., Brown, D.L., Carbone, I., Milgroom, M.G., 2017. Balancing selection for aflatoxin in Aspergillus flavus is maintained through interference competition with, and fungivory by insects. Proceedings of the Royal Society B: Biological Sciences 284, 20172408. https://doi.org/10.1098/rspb.2017.2408

Eljounaidi, K., Lee, S.K., Bae, H., 2016. Bacterial endophytes as potential biocontrol agents of vascular wilt diseases – Review and future prospects. Biological Control 103, 62–68.

https://doi.org/10.1016/j.biocontrol.2016.07.013

Fischer, G.J., Keller, N.P., 2016. Production of cross-kingdom oxylipins by pathogenic fungi: An update on their role in development and pathogenicity. Journal of Microbiology 54, 254–264. https://doi.org/10.1007/s12275-016-5620-z

Gouy, M., Guindon, S., Gascuel, O., 2010. SeaView Version 4: A Multiplatform Graphical User Interface for Sequence Alignment and Phylogenetic Tree Building. Mol Biol Evol 27, 221–224. https://doi.org/10.1093/molbev/msp259

Hamill, R.L., Higgens, C.E., Boaz, H.E., Gorman, M., 1969. The structure op beauvericin, a new depsipeptide antibiotic toxic to. Tetrahedron Letters 10, 4255–4258. https://doi.org/10.1016/S0040-4039(01)88668-8

Hardoim, P.R., van Overbeek, L.S., Berg, G., Pirttilä, A.M., Compant, S., Campisano, A., Döring, M., Sessitsch, A., 2015. The Hidden World within Plants: Ecological and Evolutionary Considerations for Defining Functioning of Microbial Endophytes. Microbiology and Molecular Biology Reviews 79, 293–320. https://doi.org/10.1128/MMBR.00050-14

Hellemans, J., Mortier, G., De Paepe, A., Speleman, F., Vandesompele, J., 2007. qBase relative quantification framework and software for management and automated analysis of real-time quantitative PCR data. Genome Biol 8, R19. https://doi.org/10.1186/gb-2007-8-2-r19

Heshof, R., Jylhä, S., Haarmann, T., Jørgensen, A.L.W., Dalsgaard, T.K., de Graaff, L.H., 2014. A novel class of fungal lipoxygenases. Applied Microbiology and Biotechnology 98, 1261–1270. https://doi.org/10.1007/s00253-013-5392-x

Hill, J., Donald, K.A., Griffiths, D.E., Donald, G., 1991. DMSO-enhanced whole cell yeast transformation. Nucleic Acids Res 19, 5791.

Hörnsten, L., Su, C., Osbourn, A.E., Hellman, U., Oliw, E.H., 2002. Cloning of the manganese lipoxygenase gene reveals homology with the lipoxygenase gene family. European Journal of Biochemistry 269, 2690–2697. https://doi.org/10.1046/j.1432-1033.2002.02936.x

Horowitz Brown, S., Zarnowski, R., Sharpee, W.C., Keller, N.P., 2008. Morphological transitions governed by density dependence and lipoxygenase activity in Aspergillus flavus. Appl. Environ. Microbiol. 74, 5674–5685. https://doi.org/10.1128/AEM.00565-08

Ivanov, I., Heydeck, D., Hofheinz, K., Roffeis, J., O'Donnell, V.B., Kuhn, H., Walther, M., 2010. Molecular enzymology of lipoxygenases. Archives of Biochemistry and Biophysics 503, 161–174. https://doi.org/10.1016/j.abb.2010.08.016

Jonkers, W., Rodriguez Estrada, A.E., Lee, K., Breakspear, A., May, G., Kistler, H.C., 2012. Metabolome and Transcriptome of the Interaction between Ustilago maydis and Fusarium verticillioides *In Vitro*. Applied and Environmental Microbiology 78, 3656–3667. https://doi.org/10.1128/AEM.07841-11

Joubert, A., Calmes, B., Berruyer, R., Pihet, M., Bouchara, J.-P., Simoneau, P., Guillemette, T., 2010. Laser nephelometry applied in an automated microplate system to study filamentous fungus growth. BioTechniques 48, 399–404. https://doi.org/10.2144/000113399

Kandel, S.L., Firrincieli, A., Joubert, P.M., Okubara, P.A., Leston, N.D., McGeorge, K.M., Mugnozza, G.S., Harfouche, A., Kim, S.-H., Doty, S.L., 2017. An In vitro Study of Bio-Control and Plant Growth Promotion Potential of Salicaceae Endophytes. Front Microbiol 8, 386.

https://doi.org/10.3389/fmicb.2017.00386

Kühn, H., Wiesner, R., Rathmann, J., Schewe, T., 1991. Formation of ketodienoic fatty acids by the pure pea lipoxygenase-1. Eicosanoids 4, 9–14.

Kuribayashi, T., Kaise, H., Uno, C., Hara, T., Hayakawa, T., Joh, T., 2002. Purification and Characterization of Lipoxygenase from Pleurotus ostreatus. J. Agric. Food Chem. 50, 1247–1253. https://doi.org/10.1021/jf0112217

Langenfeld, A., Prado, S., Nay, B., Cruaud, C., Lacoste, S., Bury, E., Hachette, F., Hosoya, T., Dupont, J., 2013. Geographic locality greatly influences fungal endophyte communities in Cephalotaxus harringtonia. Fungal Biology 117, 124–136. https://doi.org/10.1016/j.funbio.2012.12.005

Latz, M.A.C., Jensen, B., Collinge, D.B., Jørgensen, H.J.L., 2018. Endophytic fungi as biocontrol agents: elucidating mechanisms in disease suppression. Plant Ecology & Diversity 11, 555–567. https://doi.org/10.1080/17550874.2018.1534146

López-Berges, M.S., Hera, C., Sulyok, M., Schäfer, K., Capilla, J., Guarro, J., Di Pietro, A., 2013. The velvet complex governs mycotoxin production and virulence of *Fusarium oxysporum* on plant and mammalian hosts: Velvet governs mycotoxins and virulence in *Fusarium*. Molecular Microbiology 87, 49–65. https://doi.org/10.1111/mmi.12082

Mashima, R., Okuyama, T., 2015. The role of lipoxygenases in pathophysiology; new insights and future perspectives. Redox Biology 6, 297–310. https://doi.org/10.1016/j.redox.2015.08.006

Michielse, C.B., Rep, M., 2009. Pathogen profile update: *Fusarium oxysporum*. Molecular Plant Pathology 10, 311–324. https://doi.org/10.1111/j.1364-3703.2009.00538.x

Noverr, M.C., Erb-Downward, J.R., Huffnagle, G.B., 2003. Production of Eicosanoids and Other Oxylipins by Pathogenic Eukaryotic Microbes. Clinical Microbiology Reviews 16, 517–533. https://doi.org/10.1128/CMR.16.3.517-533.2003

Oliw, E.H., 2002. Plant and fungal lipoxygenases. Prostaglandins & other lipid mediators 68, 313–323.

Paciolla, C., Dipierro, N., Mulè, G., Logrieco, A., Dipierro, S., 2004. The mycotoxins beauvericin and T-2 induce cell death and alteration to the ascorbate metabolism in tomato protoplasts. Physiological and Molecular Plant Pathology 65, 49–56. https://doi.org/10.1016/j.pmpp.2004.07.006

Partida-Martínez, L.P., Heil, M., 2011. The microbe-free plant: fact or artifact? Front Plant Sci 2, 100. https://doi.org/10.3389/fpls.2011.00100

Petrini, O., 1991. Fungal Endophytes of Tree Leaves, in: Andrews, J.H., Hirano, S.S. (Eds.), Microbial Ecology of Leaves, Brock/Springer Series in Contemporary Bioscience. Springer New York, pp. 179–197.

Peyraud, R., Dubiella, U., Barbacci, A., Genin, S., Raffaele, S., Roby, D., 2017. Advances on plant-pathogen interactions from molecular toward systems biology perspectives. The Plant Journal 90, 720–737. https://doi.org/10.1111/tpj.13429

Pohl, C., Kock, J., 2014. Oxidized Fatty Acids as Inter-Kingdom Signaling Molecules. Molecules 19, 1273–1285. https://doi.org/10.3390/molecules19011273

Rodriguez Estrada, A.E., Hegeman, A., Corby Kistler, H., May, G., 2011. In vitro interactions between Fusarium verticillioides and Ustilago maydis through real-time PCR and metabolic profiling. Fungal Genetics and Biology 48, 874–885. https://doi.org/10.1016/j.fgb.2011.06.006

Rodriguez, R.J., Henson, J., Van Volkenburgh, E., Hoy, M., Wright, L., Beckwith, F., Kim, Y.-O., Redman, R.S., 2008. Stress tolerance in plants via habitat-adapted symbiosis. The ISME Journal 2, 404–416. https://doi.org/10.1038/ismej.2007.106

Rodriguez, R.J., White Jr, J.F., Arnold, A.E., Redman, R.S., 2009. Fungal endophytes: diversity and functional roles. New Phytologist 182, 314–330. https://doi.org/10.1111/j.1469-8137.2009.02773.x

Scarpari, M., Punelli, M., Scala, V., Zaccaria, M., Nobili, C., Ludovici, M., Camera, E., Fabbri, A.A., Reverberi, M., Fanelli, C., 2014. Lipids in Aspergillus flavus-maize interaction. Frontiers in Microbiology 5. https://doi.org/10.3389/fmicb.2014.00074

Šišić, A., Baćanović, J., Finckh, M.R., 2017. Endophytic Fusarium equiseti stimulates plant growth and reduces root rot disease of pea (Pisum sativum L.) caused by Fusarium avenaceum and Peyronellaea pinodella. European Journal of Plant Pathology 148, 271–282. https://doi.org/10.1007/s10658-016-1086-4

Spraker, J.E., Wiemann, P., Baccile, J.A., Venkatesh, N., Schumacher, J., Schroeder, F.C., Sanchez, L.M., Keller, N.P., 2018. Conserved Responses in a War of Small Molecules between a Plant-Pathogenic Bacterium and Fungi. mBio 9. https://doi.org/10.1128/mBio.00820-18

Su, C., Oliw, E.H., 1998. Manganese Lipoxygenase: PURIFICATION AND CHARACTERIZATION. Journal of Biological Chemistry 273, 13072–13079. https://doi.org/10.1074/jbc.273.21.13072

Tian, Y., Amand, S., Buisson, D., Kunz, C., Hachette, F., Dupont, J., Nay, B., Prado, S., 2014. The fungal leaf endophyte Paraconiothyrium variabile specifically metabolizes the host-plant metabolome for its own benefit. Phytochemistry 108, 95–101. https://doi.org/10.1016/j.phytochem.2014.09.021

Tsitsigiannis, D.I., Keller, N.P., 2007. Oxylipins as developmental and host–fungal communication signals. Trends in Microbiology 15, 109–118. https://doi.org/10.1016/j.tim.2007.01.005

Upadhyay, Handa, Mattoo, 2019. Transcript Abundance Patterns of 9- and 13-Lipoxygenase Subfamily Gene Members in Response to Abiotic Stresses (Heat, Cold, Drought or Salt) in Tomato (Solanum lycopersicum L.) Highlights Member-Specific Dynamics Relevant to Each Stress. Genes 10, 683. https://doi.org/10.3390/genes10090683

Vallet, M., Vanbellingen, Q.P., Fu, T., Le Caer, J.-P., Della-Negra, S., Touboul, D., Duncan, K.R., Nay, B., Brunelle, A., Prado, S., 2017. An Integrative Approach to Decipher the Chemical Antagonism between the Competing Endophytes Paraconiothyrium variabile and Bacillus subtilis. J. Nat. Prod. 80, 2863–2873. https://doi.org/10.1021/acs.jnatprod.6b01185

Vandenkoornhuyse, P., Quaiser, A., Duhamel, M., Van, A.L., Dufresne, A., 2015. The importance of the microbiome of the plant holobiont. New Phytologist 206, 1196–1206. https://doi.org/10.1111/nph.13312

Venkatesh, N., Keller, N.P., 2019. Mycotoxins in Conversation With Bacteria and Fungi. Frontiers in Microbiology 10. https://doi.org/10.3389/fmicb.2019.00403

Waller, F., Achatz, B., Baltruschat, H., Fodor, J., Becker, K., Fischer, M., Heier, T., Hückelhoven, R., Neumann, C., von Wettstein, D., others, 2005. The endophytic fungus Piriformospora indica reprograms barley to salt-stress tolerance, disease resistance, and higher yield. Proceedings of the National Academy of Sciences of the United States of America 102, 13386–13391.

Wang, Q., Xu, L., 2012. Beauvericin, a Bioactive Compound Produced by Fungi: A Short Review. Molecules 17, 2367–2377. https://doi.org/10.3390/molecules17032367

Wasternack, C., Forner, S., Strnad, M., Hause, B., 2013. Jasmonates in flower and seed development. Biochimie 95, 79–85. https://doi.org/10.1016/j.biochi.2012.06.005

Wennman, A., Magnuson, A., Hamberg, M., Oliw, E.H., 2015. Manganese lipoxygenase of F. oxysporum and the structural basis for biosynthesis of distinct 11-hydroperoxy stereoisomers. J Lipid Res 56, 1606–1615. https://doi.org/10.1194/jlr.M060178

Wennman, A., Oliw, E.H., 2013. Secretion of two novel enzymes, manganese 9S-lipoxygenase and epoxy alcohol synthase, by the rice pathogen Magnaporthe salvinii. The Journal of Lipid Research 54, 762–775. https://doi.org/10.1194/jlr.M033787

Wilson, D., 1995. Endophyte: The Evolution of a Term, and Clarification of Its Use and Definition. Oikos 73, 274. https://doi.org/10.2307/3545919

Winter, D.J., 2017. rentrez: An R package for the NCBI eUtils API 9, 7.

Zhang, L., Yan, K., Zhang, Y., Huang, R., Bian, J., Zheng, C., Sun, H., Chen, Z., Sun, N., An, R., Min, F., Zhao, W., Zhuo, Y., You, J., Song, Y., Yu, Z., Liu, Z., Yang, K., Gao, H., Dai, H., Zhang, X., Wang, J., Fu, C., Pei, G., Liu, J., Zhang, S., Goodfellow, M., Jiang, Y., Kuai, J., Zhou, G., Chen, X., 2007. High-throughput synergy screening identifies microbial metabolites as combination agents for the treatment of fungal infections. Proc Natl Acad Sci U S A 104, 4606–4611. https://doi.org/10.1073/pnas.0609370104

Zhu, D., Zhong, X., Tan, R., Chen, L., Huang, G., Li, J., Sun, X., Xu, L., Chen, J., Ou, Y., Zhang, T., Yuan, D., Zhang, Z., Shu, W., Ma, L., 2010. High-throughput cloning of human liver complete open reading frames using homologous recombination in Escherichia coli. Analytical Biochemistry 397, 162–167. https://doi.org/10.1016/j.ab.2009.10.018